SAM transmethylation pathway and adenosine recycling to ATP are essential for systemic regulation and immune response

Pavla Nedbalova[1], Nikola Kaislerova[1], Lenka Chodakova[1], Martin Moos[2,3,#], Tomas Dolezal[1,#]

[1] Department of Molecular Biology and Genetics, Faculty of Science, University of South Bohemia, České Budějovice, Czech Republic

[2] Laboratory of Analytical Biochemistry and Metabolomics, Institute of Entomology, Biology Centre, Czech Academy of Sciences, České Budějovice, Czech Republic

[3] Department of Applied Chemistry, Faculty of Agriculture and Technology, University of South Bohemia, České Budějovice, Czech Republic,

Corresponding author - MM: moos@bclab.eu, TD: tomas.dolezal@prf.jcu.cz

ABSTRACT

During parasitoid wasp infection, activated immune cells of *Drosophila melanogaster* larvae release adenosine to conserve nutrients for immune response. S-adenosylmethionine (SAM) is a methyl group donor for most methylations in the cell and is synthesized from methionine and ATP. After methylation, SAM is converted to S-adenosylhomocysteine, which is further metabolized to adenosine and homocysteine. Here, we show that the SAM transmethylation pathway is up-regulated during immune cell activation and that the adenosine produced by this pathway in immune cells acts as a systemic signal to delay *Drosophila* larval development and ensure sufficient nutrient supply to the immune system. We further show that the up-regulation of the SAM transmethylation pathway and the efficiency of the immune response also depend on the recycling of adenosine back to ATP by adenosine kinase and adenylate kinase. We therefore hypothesize that adenosine may act as a sensitive sensor of the balance between cell activity, represented by the sum of methylation events in the cell, and nutrient supply. If the supply of nutrients is insufficient for a given activity, adenosine may not be effectively recycled back into ATP and may be pushed out of the cell to serve as a signal to demand more nutrients.

Keywords:

SAM transmethylation pathway, adenosine signaling, privileged immunity, Drosophila, S-adenosylhomocysteinase, adenosine kinase, adenylate kinase

INTRODUCTION

Upon activation, immune cells fundamentally change their metabolism, requiring an increased supply of nutrients, which is essential for their effective function. Additional nutrients are delivered to immune cells by redirecting metabolites away from other tissues, making the immune system metabolically privileged, or selfish within an organism. The concept of selfish immunity proposes insulin resistance as a mechanism by which activated immune cells ensure adequate nutrient supply (Straub 2014; Dolezal 2015; Krejčová et al. 2023). For example, we have recently shown that immune cells produce cytokines Upd2 and Upd3, which induce the production of the insulin signaling inhibitor Impl2 in muscle tissue via the Jak/Stat signaling pathway. Impl2 reduces the consumption of carbohydrates by muscle, making nutrients more available to immune cells (McMullen et al. 2024). Another mechanism by which immune cells gain privileged access to nutrients is through the release of adenosine. Extracellular adenosine signaling, through the adenosine receptor, reduces nutrient consumption by non-immune tissues and slows the development of the organism, again leaving more nutrients available for the immune system (Bajgar et al. 2015; Dolezal 2015; Bajgar and Dolezal 2018).

Adenosine signaling plays a variety of roles, especially in more complex organisms such as mammals. However, the release of adenosine as a signaling molecule from cells plays a universal role from the most primitive organisms, such as social bacteria, to humans (Newby 1984; Boison and Jarvis 2021). The release of adenosine is an indication of metabolic stress and signals to neighbouring cells to adjust their behaviour accordingly. For example, the bacterium *Myxococcus xanthus* responds to nutrient depletion by releasing adenosine, which initiates the aggregation of bacteria into fruiting bodies (Shimkets and Dworkin 1981). In mammals the heart muscles secrete adenosine during ischemia, which causes blood vessels to dilate to increase blood flow and delivery of oxygen and nutrients (Lloyd et al. 1988; Deussen 1989; Kroll, Deussen, and Sweet 1992; Reiss et al. 2019). Adenosine also plays an important role in the induction of sleep, torpor and hibernation, physiological states associated with energy conservation (Fredholm, Johansson, and Wang 2011; Boison and Jarvis 2021). Therefore, the use of extracellular adenosine by immune cells to suppress nutrient consumption in non-immune tissues, thereby conserving energy for the immune response, fits well with this evolutionarily conserved role of adenosine signaling.

Adenosine is produced intracellularly in two ways (Figure 1), by conversion from AMP by nucleotidases or in the S-adenosylmethionine (SAM) transmethylation pathway from S-adenosylhomocysteine (SAH) by S-adenosylhomocysteinase (Ahcy). The increase in AMP mainly reflects the lack of energy and metabolic stress. Cells use adenylate kinase to produce one ATP and one AMP from two ADP molecules. Increased AMP activates AMPK, which suppresses energy-consuming processes in the cell and activates energy-producing processes (Kloor and Osswald 2004; P. Dzeja and Terzic 2009). AMP is also converted by nucleotidases to adenosine, which is released from the cell via the equilibrative nucleoside transporter (ENT), where it signals the metabolic stress of the cell to surrounding cells and tissues via adenosine receptors (Dolezelova et al. 2007; Fenckova et al. 2011). This is typical of cells during ischemia when they are deprived of nutrients (Deussen 1989; Schädlich et al. 2023). Since activated AMPK suppresses the function of immune cells (Salminen, Hyttinen, and Kaarniranta 2011), we would expect that in the absence of nutrients and decreasing ATP levels, the accumulated AMP would be converted to adenosine and released from the cells, thus demanding a greater supply of nutrients.

In the SAM transmethylation pathway, ATP and methionine combine to produce SAM, which is the major methyl group donor for most methylations in the cell. The SAM transmethylation pathway is one of the largest consumers of ATP when the adenosyl moiety of ATP is incorporated into SAM (i.e., it is not a conversion of ATP to ADP as in energy transfer). After the methyl group is transferred to the target molecule by methyltransferase, SAM becomes SAH, which must be rapidly converted to homocysteine and adenosine, or it will block further methylation. As methylation increases in the cell, more SAM is formed and at the same time SAH is cleared more rapidly, leading to an increase in the SAM:SAH ratio, known as the methylation index. SAH is converted to homocysteine and adenosine by Ahcy, which works in both directions; for the "SAM to homocysteine + adenosine" direction to prevail, homocysteine and adenosine must also be metabolized or excreted from the cell very rapidly (Lu 2000; Kloor and Osswald 2004; Yu et al. 2019; Roy et al. 2020; Vizán, Di Croce, and Aranda 2021).

Homocysteine can either be recycled back to methionine, or further metabolized in the transsulfuration pathway (source of cysteine, H_2S, and antioxidants) (Sbodio, Snyder, and Paul 2019). Adenosine can be catabolized to inosine by adenosine deaminase (Novakova and Dolezal 2011), or recycled to AMP by adenosine kinase and further to ATP by adenylate kinase, glycolysis or oxidative phosphorylation (R. J. Zeleznikar et al. 1990; Robert J. Zeleznikar, Dzeja, and Goldberg 1995; P. P. Dzeja, Chung, and Terzic 2007; P. Dzeja and Terzic 2009). The importance of adenosine recycling to AMP by adenosine kinase is indicated by the dependence of the methylation cycle on the concomitant function of this enzyme (Lecoq et al. 2001; Bjursell et al. 2011; Moffatt et al. 2002). Since every single methylation in the cell is associated with the formation of one adenosine molecule, the amount of adenosine accurately reflects the intensity of the SAM transmethylation pathway. In a sense, it reflects the activity of the cell, because the more processes the cell has to activate, the more new molecules it has to methylate.

We have previously shown that activated immune cells preferentially acquire nutrients during immune response by releasing adenosine, subsequently reducing nutrient uptake in non-immune tissues, thereby leading to a delay in development (Bajgar et al. 2015; Bajgar and Dolezal 2018). To elucidate the origin of adenosine in activated immune cells, we investigated the role of the SAM transmethylation pathway. Given its upregulation and critical function in mammalian immune cells (Lawson et al. 2012; Yu et al. 2019; Roy et al. 2020), we hypothesized that this pathway is also a major source of adenosine in *Drosophila* immune cells. Our results confirm that the SAM transmethylation pathway is indeed upregulated in *Drosophila* hemocytes upon parasitoid wasp infection. In addition, we show that this pathway is not only essential for the immune response, but also a source of extracellular adenosine that slows larval development. Moreover, not all adenosine is released from hemocytes, but it can be recycled back into ATP and thus re-enter the SAM transmethylation pathway.

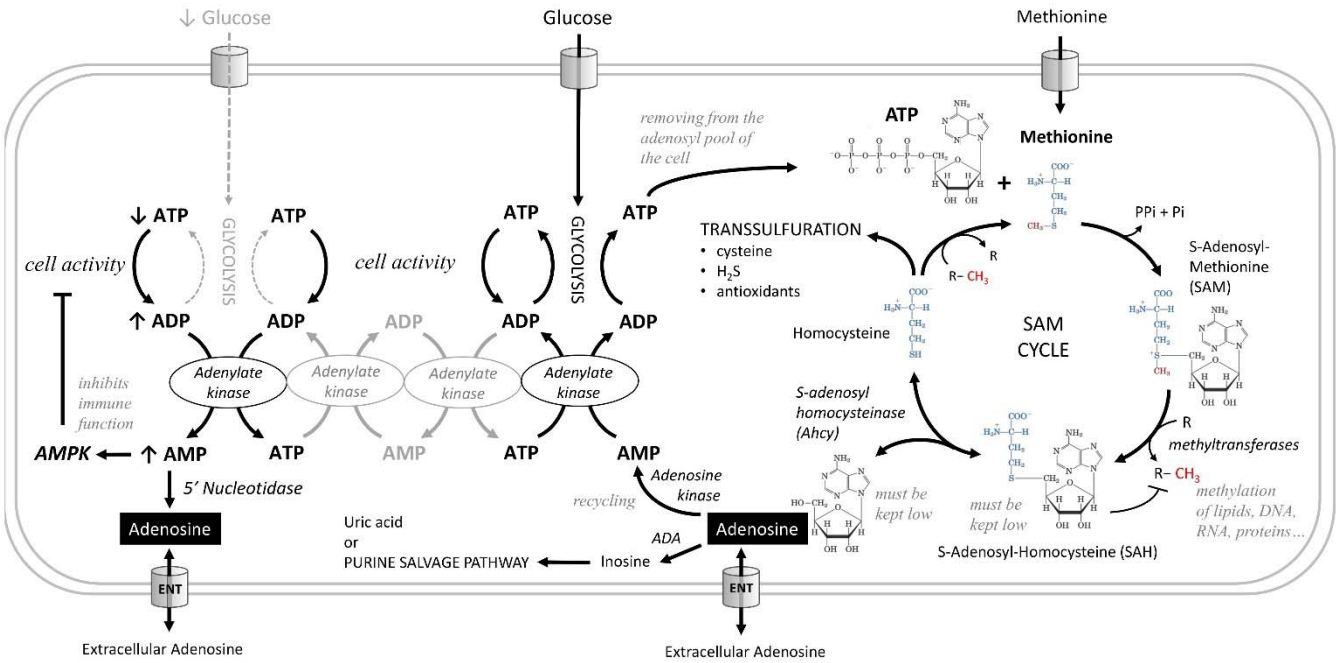

Figure 1. Metabolic pathways producing adenosine.

Adenosine can be produced from AMP by 5'-nucleotidase. AMP increases during metabolic stress, when cells use adenylate kinase to make one ATP and one AMP from two ADP molecules. Increased AMP activates AMP-activated protein kinase (AMPK), which suppresses energy-consuming processes in the cell and activates energy-producing processes, or is converted to adenosine, which can be released from cells via the equilibrative nucleoside transporter (ENT). In the S-adenosylmethionine (SAM) transmethylation pathway, the combination of ATP and methionine produces SAM, the major methyl group donor (red) for the majority of methylations that occur in the cell. During methylation, SAM is converted to S-adenosylhomocysteine (SAH), which is rapidly converted to homocysteine and adenosine by adenosylhomocysteinase (Ahcy), as it would otherwise block further methylation. Ahcy works bidirectionally, and for the "SAM to homocysteine + adenosine" direction to dominate, homocysteine and adenosine must be rapidly metabolized or cleared from the cell. Homocysteine is remethylated back to methionine or further metabolized via the transsulfuration pathway (source of cysteine, H_2S, and antioxidants). The catabolism of adenosine to inosine is mediated by adenosine deaminase (ADA) or recycled to AMP by adenosine kinase which becomes ATP through adenylate kinase, glycolysis or oxidative phosphorylation. Another possible source of adenosine is RNA degradation, which is not shown in this scheme.

127 **RESULTS**

128 **SAM transmethylation pathway accelerates in activated hemocytes**

129 One of the important sources of adenosine in hemocytes is the SAM transmethylation pathway (Figure
130 2A). Putative methionine transporters, as well as all enzymes of this pathway, are strongly expressed in
131 hemocytes, both in the resting and activated state (Figure 2B, Figure 2—figure supplement 1, S1 Data
132 and S4 Data). Methionine can be transported from the hemolymph to the cytosol by *Drosophila* L type
133 amino acid transporters orthologs mnd (CG3297; FBgn0002778), Jhl-21 (CG12317; FBgn0028425),
134 CG1607 (FBgn0039844), sbm (CG9413; FBgn0030574), or gb (CG6070; FBgn0039487). The expression of
135 *mnd* and *gb* is particularly high and is further increased during infection (Figure 2B). SAM synthetase
136 (Sam-S; CG2674; EC 2.5.1.6; FBgn0005278) converts methionine and ATP into SAM. SAM is used for
137 methylation by a wide range of methyltransferases (EC 2.1.1.-), or in polyamine synthesis, by SAM
138 decarboxylase (SamDC; CG5029; EC 4.1.1.50; FBgn0019932), producing 5'-methylthioadenosine (MTA).
139 The actual methylation, using SAM as a donor, is carried by various methyltransferases. Using our
140 RNAseq of hemocytes, we checked the expression of 200 genes (S3 Table), which are categorized as
141 *Drosophila* methyltransferases. We found that 43 methyltransferases (at least 24 of them categorized as
142 SAM-dependent methyltransferases) significantly increased their expression in both 9 and 18 hpi (Figure
143 2—figure supplement 3). Methylation reactions produce SAH, a potent inhibitor of methyltransferases
144 which must be quickly removed to keep the pathway running. Ahcy (Ahcy; CG11654; EC 3.3.1.1;
145 FBgn0014455) hydrolyzes SAH into adenosine and homocysteine and shows the highest expression
146 among SAM transmethylation pathway enzymes (Figure 2B). AhcyL1 (CG9977; FBgn0035371) and
147 AhcyL2 (CG8956; FBgn0015011), which work as dominant-negative regulators of Ahcy (Parkhitko et al.
148 2016) have a lower expression and are downregulated during infection (Figure 2B). When adenosine and
149 homocysteine accumulate, Ahcy changes the activity in favor of SAH synthesis. Thus, adenosine and
150 homocysteine must be rapidly metabolized (Kloor and Osswald 2004). Homocysteine can be
151 remethylated back to methionine, by betaine-homocysteine methyltransferase (Bhmt; CG10623; EC
152 2.1.1.5; FBgn0032727) or homocysteine S-methyltransferase (CG10621; EC 2.1.1.10; FBgn0032726).
153 Alternatively, it is used as a substrate for Cystathionine β-synthase (Cbs; CG1753; EC 4.2.1.22;
154 FBgn0031148) to produce cystathionine (CTH) in the transsulfuration pathway (Figure 2A). Overall,
155 enzymes of the SAM transmethylation pathway, and its associated metabolic branches, are strongly
156 expressed in hemocytes (Figure 2B) and possible increase in SAM transmethylation pathway can be
157 suggested from RNAseq data (1) by increased expression of 4 transporters capable of transporting
158 methionine, (2) by decreased expression of AhcyL2 (dominant-negative regulator of Ahcy) and (3) by
159 increased expression of 43 out of 200 methyltransferases. Nevertheless, the actual metabolism cannot
160 be determined based solely on the gene expression.

161 To analyze SAM transmethylation pathway metabolism, we used high pressure liquid chromatography
162 coupled with tandem mass spectrometry (HPLC-MS/MS). In addition to detecting relative levels of
163 metabolites, 13C-labeled methionine tracing was used to determine methionine usage in the SAM
164 transmethylation pathway in hemocytes of infection and non-infected animals. Hemocytes were
165 extracted by bleeding larvae at 20 hours post infection (hpi). Cells were incubated in media containing
166 0,33 µM $^{13}C_5$ methionine for 20 minutes. This *ex vivo* incubation was designed to resemble physiological
167 conditions. In control larvae, the labeled intracellular methionine fraction reached almost 70% in resting
168 hemocytes and over 80% in activated hemocytes after 20 min of *ex vivo* incubation, demonstrating a
169 substantial uptake of methionine into hemocytes (Figure 2C). Much of this methionine is used for SAM

170 production and methylation, as indicated by the 2-fold increase of SAM and SAH in infected compared
171 to control animals (Figure 2D and E); demonstrating an upregulation of the SAM transmethylation
172 pathway in activated hemocytes. This is further supported by a significantly higher methylation index
173 (ratio of SAM:SAH; Figure 2H-J) in activated hemocytes.

174 SAH is cleaved into homocysteine and adenosine, however, we were unable to reliably detect
175 homocysteine in our metabolomic analysis. Homocysteine can be recycled back to methionine, to enter
176 another round of the SAM transmethylation pathway. In this scenario, fully labeled 13C5 methionine, as
177 was used in this assay, would lead to the formation of methionine m+4. One labeled carbon is used in
178 the methylation reaction while the unlabeled methyl group would be added during recycling (Figure 2A).
179 However, the m+4 portion of the labeled methionine (m+4 and m+5) did not exceed the 3% threshold,
180 set by the methionine labeling impurity (ratio "m+4/[m+4 + m+5]" in the medium was 3%; Figure 2F).
181 This indicates that methionine used for the SAM transmethylation pathway in hemocytes is derived
182 from hemolymph and homocysteine is not remethylated to methionine.

183 To investigate the role of the SAM transmethylation pathway in hemocytes, we knocked down Ahcy by
184 hemocyte-specific RNAi (Figure 2—figure supplement 1 and 2). Ahcy RNAi leads to reduced 13C-labeled
185 methionine uptake in resting hemocytes, although uptake is still increased upon infection (Figure 2C).
186 Methionine incorporation into SAM is significantly lower in activated hemocytes (Figure 2D) and
187 incorporation into SAH is decreased in both, quiescent and activated hemocytes (Figure 2E). These
188 results imply that the SAM transmethylation pathway slows down when there is insufficient Ahcy
189 available. This is reflected in metabolite levels, where SAH is heavily accumulated in Ahcy RNAi
190 hemocytes (Figure 2I) and SAM and methionine levels are higher compared to controls (Figure 2G and
191 H); indicating that they are not metabolized in the SAM transmethylation pathway. This is substantiated
192 by a methylation index that is very low compared to controls, and does not increase upon infection
193 (Figure 2J).

194 SAM can also be utilized for polyamine synthesis that, in addition to polyamines, produces 5-
195 methylthioadenosine (MTA). Polyamines are essential for cell growth and proliferation and participate in
196 various cellular processes (replication, gene expression, biomolecules modifications, etc.). They play a
197 role in macrophage polarization and regulation (Latour, Gobert, and Wilson 2020; Xuan et al. 2023).
198 There is significantly higher incorporation of 13C methionine into MTA in activated hemocytes (Figure
199 2K) with no changes in MTA level (Figure 2L). Ahcy RNAi hemocytes have increased MTA levels (Figure
200 2L), which can reflect MTA accumulation, due to decreased SAM transmethylation pathway activity.
201 Decreased 13C methionine incorporation into MTA upon Ahcy knockdown by RNAi (Figure 2K) may be
202 caused by dilution, as unlabeled MTA accumulate (Figure 2L) therefore, we are unable to determine the
203 effect of Ahcy RNAi on polyamine synthesis.

204 The SAM transmethylation pathway is connected to the transsulfuration pathway, which produces
205 cysteine and further antioxidants taurine, and glutathione (Sbodio, Snyder, and Paul 2019). The
206 transsulfuration pathway is one of the ways to metabolically remove homocysteine produced by Ahcy
207 when Cbs converts homocysteine into CTH. This is supported by notable 13C methionine incorporation
208 into CTH (Figure 2M). Interestingly, there is a small, but significant, drop in the labeled CTH fraction in
209 activated hemocytes (Figure 2M), however, this could be due to an overall increase in the level of CTH,
210 including the unlabeled form (Figure 2N). As reported above, the SAM transmethylation pathway is
211 accelerated in activated hemocytes, producing more adenosine, as well as more homocysteine, which

212 must be removed to keep the pathway running. Cystathionine γ-lyase (Cth; CG5345; EC 4.4.1.1;
213 FBgn0000566) usually converts CTH to cysteine. However, this enzyme can also use homocysteine for
214 H_2S production, and was shown to be responsible for homocysteine removal under
215 hyperhomocysteinemia, when Cbs is unresponsive (Singh et al. 2009). H_2S has many diverse roles in the
216 organismal physiology, dependent on its source, localization, and concentration, and has already been
217 connected with immune cells (Sbodio, Snyder, and Paul 2019; Dilek et al. 2020). Based on our
218 transcriptomic data, *Cbs* expression in *Drosophila* larval hemocytes is rather low, and even decreases
219 during infection. Interestingly, cystathionine γ-lyase is strongly expressed, at similar levels to Ahcy.
220 Therefore, our data gives evidence to the clearance of homocysteine by cystathionine γ-lyase and H_2S
221 production rather than via CTH and Cbs.

222 Knockdown of Ahcy leads to the accumulation of SAH and thus the production of homocysteine, the
223 substrate for CTH, should be strongly inhibited. However, our data shows the relative levels of
224 methionine, as well as the incorporation of 13C methionine into CTH in Ahcy RNAi hemocytes is
225 equivalent to controls (Figure 2M and N). This suggests, there is an alternative connection of methionine
226 with homocysteine and consequently CTH, in addition to Ahcy. Uncovering this alternative connection
227 would be of interest, although it is beyond the scope of this current work.

228 In summary, activated hemocytes increase the uptake of methionine to ramp up the transmethylation
229 pathway. SAM is not only a substrate for methylation, but is also used for polyamine synthesis.
230 Homocysteine is not recycled back to methionine, but is further metabolized in the transsulfuration
231 pathway. Interestingly, our data suggest an alternative link between methionine and CTH independent
232 of Ahcy. Hemocyte-specific Ahcy-RNAi potently suppresses the SAM transmethylation pathway.

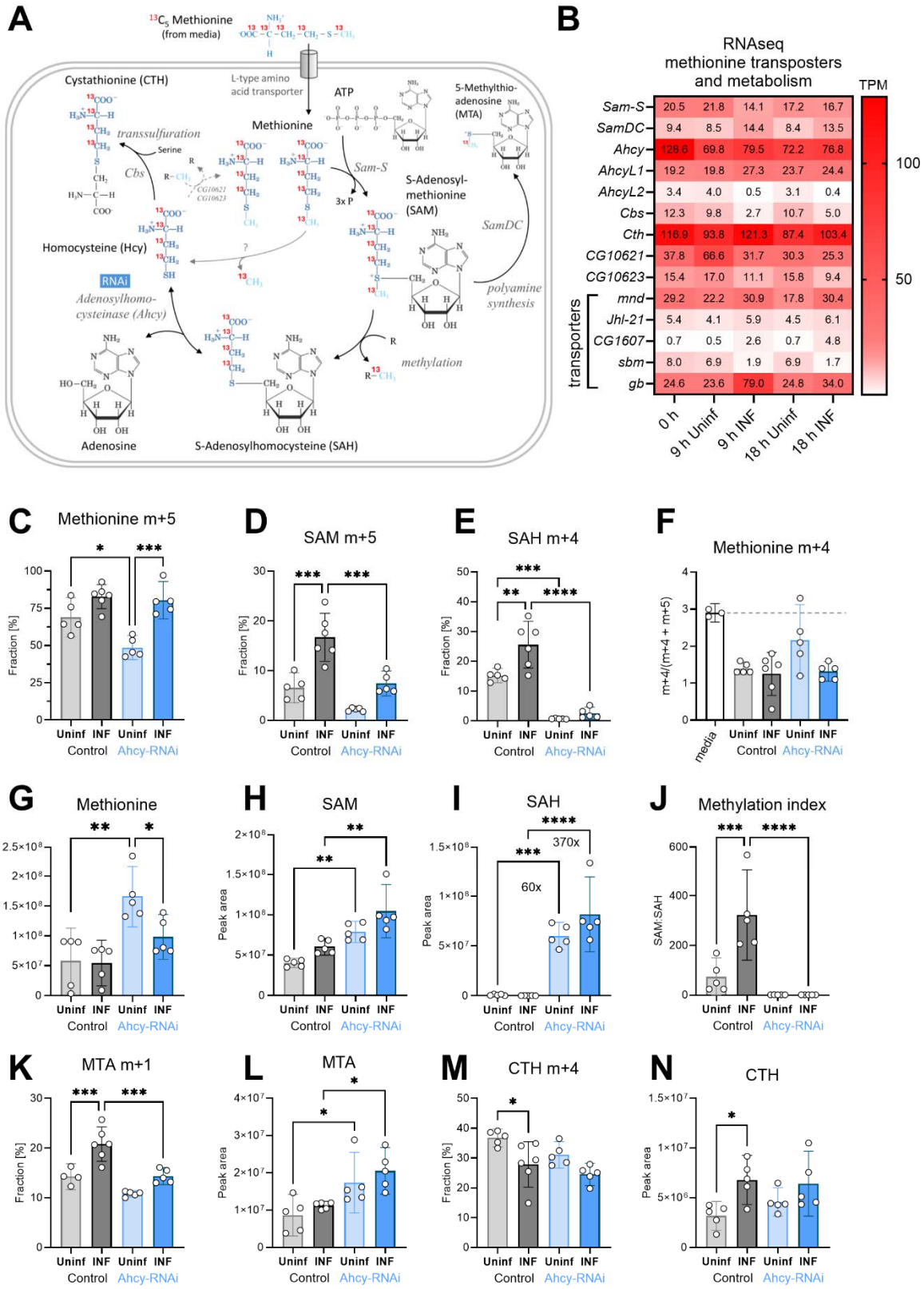
A
13C5 Methionine (from media)
L-type amino acid transporter
Cystathionine (CTH)
ATP
5-Methylthio-adenosine (MTA)
Methionine
transsulfuration
Serine
Cbs
Sam-S
3x P
S-Adenosyl-methionine (SAM)
SamDC
Homocysteine (Hcy)
RNAi
Adenosylhomo-cysteinase (Ahcy)
polyamine synthesis
methylation
Adenosine
S-Adenosylhomocysteine (SAH)
B
RNAseq methionine transposters and metabolism
TPM
Sam-S 20.5 21.8 14.1 17.2 16.7
SamDC 9.4 8.5 14.4 8.4 13.5
Ahcy 128.6 69.8 79.5 72.2 76.8
AhcyL1 19.2 19.8 27.3 23.7 24.4
AhcyL2 3.4 4.0 0.5 3.1 0.4
Cbs 12.3 9.8 2.7 10.7 5.0
Cth 116.9 93.8 121.3 87.4 103.4
CG10621 37.8 66.6 31.7 30.3 25.3
CG10623 15.4 17.0 11.1 15.8 9.4
transporters
mnd 29.2 22.2 30.9 17.8 30.4
Jhl-21 5.4 4.1 5.9 4.5 6.1
CG1607 0.7 0.5 2.6 0.7 4.8
sbm 8.0 6.9 1.9 6.9 1.7
gb 24.6 23.6 79.0 24.8 34.0
100
50
0 h
9 h Uninf
9 h INF
18 h Uninf
18 h INF
C Methionine m+5
Fraction [%]
D SAM m+5
Fraction [%]
E SAH m+4
Fraction [%]
F Methionine m+4
m+4/(m+4 + m+5)
media
G Methionine
Peak area
H SAM
Peak area
I SAH
Peak area
370x
60x
J Methylation index
SAM:SAH
K MTA m+1
Fraction [%]
L MTA
Peak area
M CTH m+4
Fraction [%]
N CTH
Peak area
Uninf INF Uninf INF
Control Ahcy-RNAi

233

234 **Figure 2. Analysis of the SAM transmethylation pathway in larval hemocytes by *ex vivo* stable ^{13}C**
235 **isotope tracing**

236 (A) Schematic representation of the SAM transmethylation pathway with polyamine synthesis and
237 transsulfuration branches and labeling with L-methionine-$^{13}C_5$ from media (red 13 represents the
238 labeled carbon). Light blue CH_3 represents the methyl group used during transmethylation or
239 remethylation. Enzymes and processes are italicized. RNAi in blue rectangle represents
240 adenosylhomocysteinase knockdown. (B) Expression heat map (bulk RNAseq) of methionine
241 transporters and enzymes in circulating hemocytes from uninfected (Uninf) and infected (INF) third
242 instar larvae collected at 0, 9 and 18 hpi (0 hpi = 72 hours after egg laying). Means of 6 replicates (10
243 replicates in case of 18 h INF) shown in each cell are transcripts per million (TPM) - for comparison, only
244 20% of genes in RNAseq show expression higher than 15 TPM (data in S1_Data and S4_Data). (C-E,K,M)
245 ^{13}C-labeling of metabolites in hemocytes, which were incubated *ex vivo* for 20 min in media containing
246 0,33 µM L-methionine-$^{13}C_5$. The graphs show the fraction of the compound with one (m+1), four (m+4)
247 or five (m+5) ^{13}C-labeled carbons – methionine m+5 (C), S-adenosylmethionine (SAM) m+5 (D), S-
248 adenosylhomocysteine (SAH) m+4 (E), 5-methylthioadenosine (MTA) m+1 (K) and cystathionine (CTH)
249 m+4 (M). (F) Methionine m+4 portion of total labeled methionine (m+4 and m+5) in media representing
250 the labeling impurity of used methionine (white bar setting threshold - dashed line), and in hemocyte
251 samples. (G-I,L,N) Total levels of methionine (G), SAM (H), SAH (I), MTA (L) and CTH (N) in hemocytes
252 shown as the mean metabolite amounts expressed by the normalized peak area. (J) Methylation index
253 calculated as the ratio of SAM:SAH levels (peak areas in H and I). (C-N) Bars represent mean values with
254 95% CI of uninfected (Uninf, light grey) and infected (INF, dark grey) control and uninfected (Uninf, light
255 blue) and infected (INF, dark blue) Ahcy-RNAi samples; each dot represents one biological replicate
256 (numerical values in S1_Data and S2_Data); asterisks represent significant differences between samples
257 tested by ordinary one-way ANOVA Tukey's multiple comparison test (*$p<0.05$, **$p<0.01$, ***$p<0.001$,
258 ****$p<0.0001$).
259

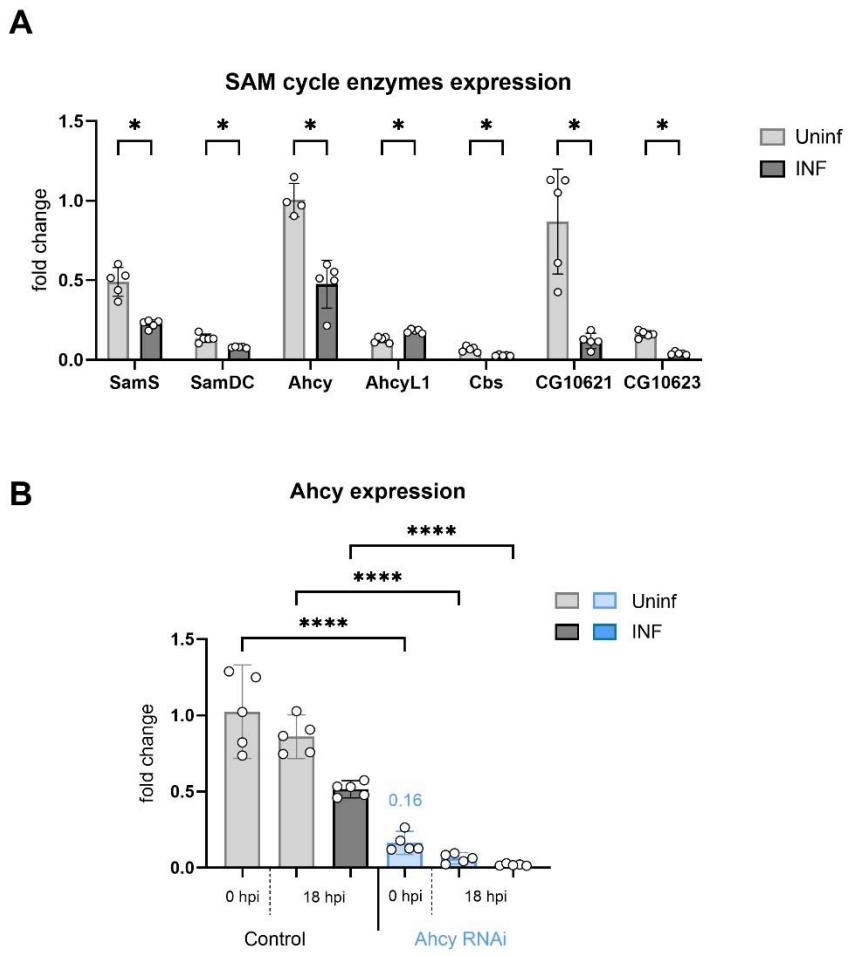

Figure 2-figure supplement 1. Expression of SAM transmethylation pathway enzymes and Ahcy RNAi

(A) Expression analysis of enzymes in the SAM transmethylation pathway in circulating hemocytes from uninfected (Uninf; light gray) and infected (INF; dark gray) third instar larvae collected at 18 hpi by RT-qPCR. Bars show fold change compared to uninfected Ahcy samples (expression levels were normalized to *RpL32* expression in each sample), each dot represents a biological replicate. Asterisks indicate significant differences between samples tested by multiple unpaired t-test. (B) Analysis of Ahcy knockdown efficiency at 0 and 18 hpi by RT-qPCR. RNAi was specifically induced in hemocytes by *SrpD-Gal4 tubP-GAL80ts* driven expression of *UAS-Ahcy-RNAi*^{HMS05799} in larvae maintained at 18°C for the first 3 days of development and then transferred to 25°C. RNAi reduces Ahcy expression to 16% of control at the onset of infection (0 h). Bars represent means with 95% CI of uninfected (Uninf, light gray) and infected (INF, dark gray) control (driver crossed to *P{CaryP}Msp300attP40* control without RNAi) and uninfected (Uninf, light blue) and infected (INF, dark blue) Ahcy-RNAi samples; each dot represents a biological replicate (numerical values in S1_Data); asterisks indicate significant differences between samples tested by ordinary one-way ANOVA Tukey's multiple comparison test (****$p<0.0001$).

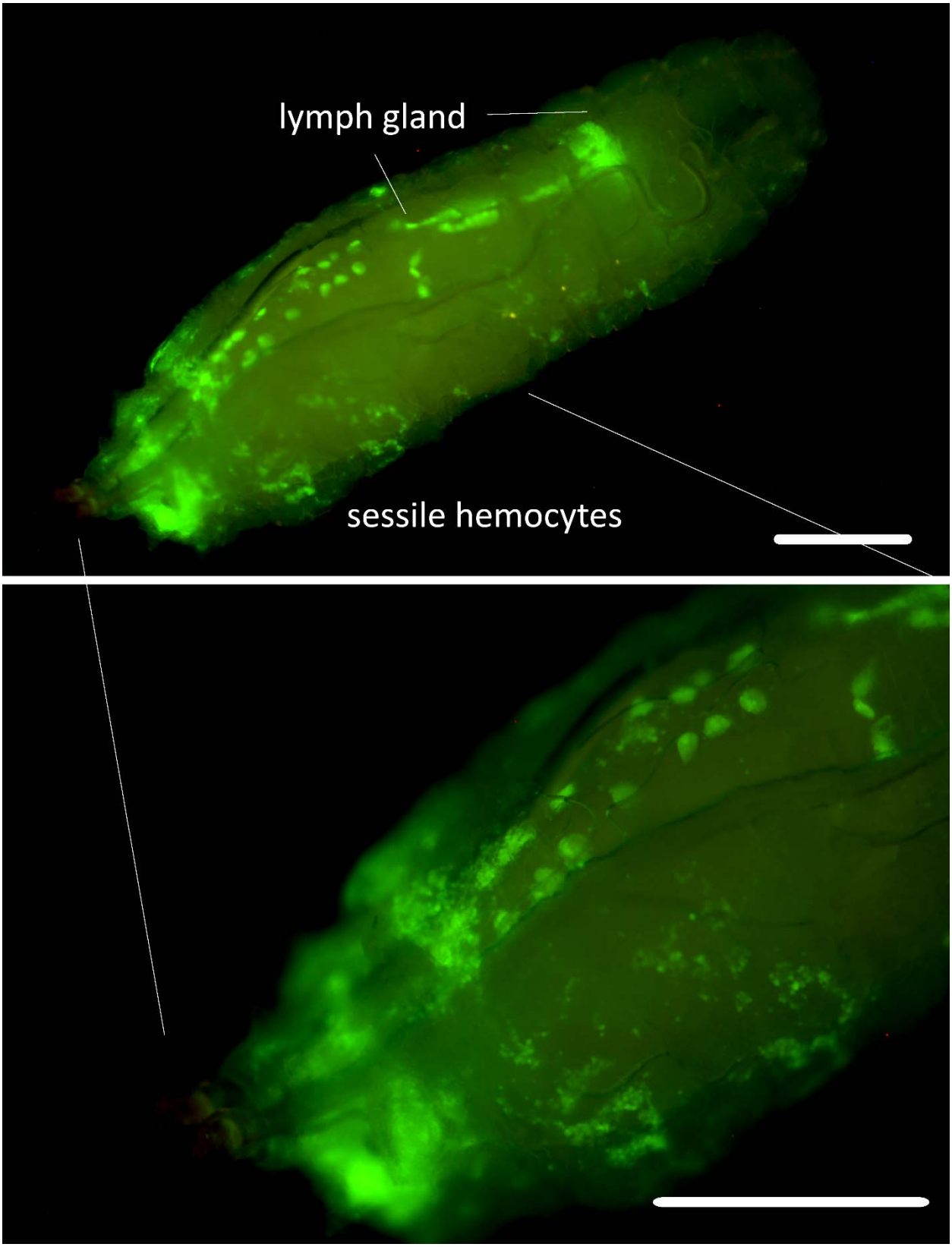

Figure 2-figure supplement 2. Srp-Gal4 Gal80 driver expression

278 *SrpD-Gal4 tubP-GAL80ts* driven expression of *UAS-GFP* in 3rd-instar larvae maintained at 18°C for the
279 first 3 days of development and then transferred to 25°C. GFP expression is detected in all lobes of
280 lymph gland, pericardial cells and circulating and sessile hemocytes. Scale bar 250 μm.

281

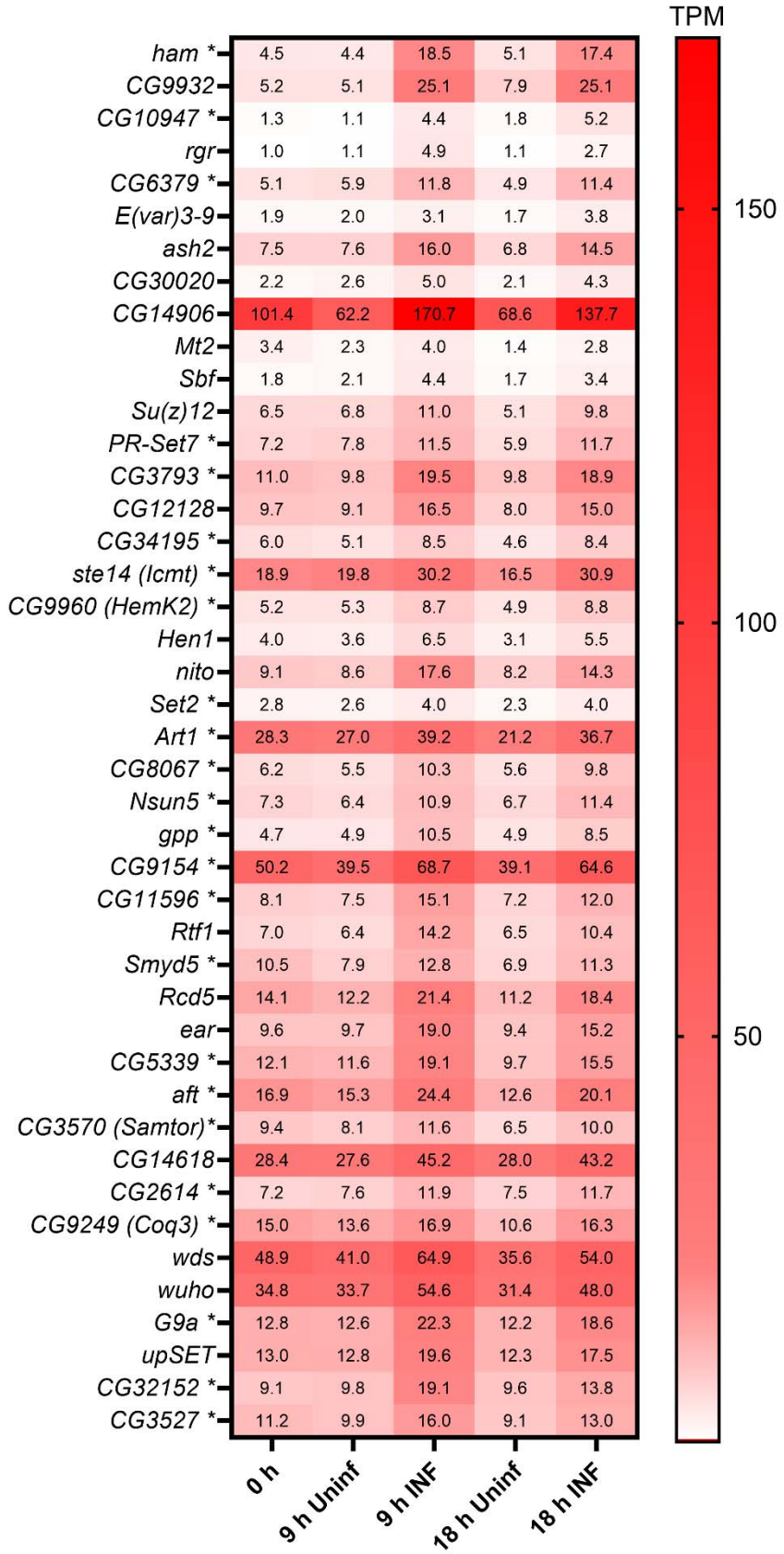

	0 h	9 h Uninf	9 h INF	18 h Uninf	18 h INF
ham *	4.5	4.4	18.5	5.1	17.4
CG9932	5.2	5.1	25.1	7.9	25.1
CG10947 *	1.3	1.1	4.4	1.8	5.2
rgr	1.0	1.1	4.9	1.1	2.7
CG6379 *	5.1	5.9	11.8	4.9	11.4
E(var)3-9	1.9	2.0	3.1	1.7	3.8
ash2	7.5	7.6	16.0	6.8	14.5
CG30020	2.2	2.6	5.0	2.1	4.3
CG14906	101.4	62.2	170.7	68.6	137.7
Mt2	3.4	2.3	4.0	1.4	2.8
Sbf	1.8	2.1	4.4	1.7	3.4
Su(z)12	6.5	6.8	11.0	5.1	9.8
PR-Set7 *	7.2	7.8	11.5	5.9	11.7
CG3793 *	11.0	9.8	19.5	9.8	18.9
CG12128	9.7	9.1	16.5	8.0	15.0
CG34195 *	6.0	5.1	8.5	4.6	8.4
ste14 (Icmt) *	18.9	19.8	30.2	16.5	30.9
CG9960 (HemK2) *	5.2	5.3	8.7	4.9	8.8
Hen1	4.0	3.6	6.5	3.1	5.5
nito	9.1	8.6	17.6	8.2	14.3
Set2 *	2.8	2.6	4.0	2.3	4.0
Art1 *	28.3	27.0	39.2	21.2	36.7
CG8067 *	6.2	5.5	10.3	5.6	9.8
Nsun5 *	7.3	6.4	10.9	6.7	11.4
gpp *	4.7	4.9	10.5	4.9	8.5
CG9154 *	50.2	39.5	68.7	39.1	64.6
CG11596 *	8.1	7.5	15.1	7.2	12.0
Rtf1	7.0	6.4	14.2	6.5	10.4
Smyd5 *	10.5	7.9	12.8	6.9	11.3
Rcd5	14.1	12.2	21.4	11.2	18.4
ear	9.6	9.7	19.0	9.4	15.2
CG5339 *	12.1	11.6	19.1	9.7	15.5
aft *	16.9	15.3	24.4	12.6	20.1
*CG3570 (Samtor)**	9.4	8.1	11.6	6.5	10.0
CG14618	28.4	27.6	45.2	28.0	43.2
CG2614 *	7.2	7.6	11.9	7.5	11.7
CG9249 (Coq3) *	15.0	13.6	16.9	10.6	16.3
wds	48.9	41.0	64.9	35.6	54.0
wuho	34.8	33.7	54.6	31.4	48.0
G9a *	12.8	12.6	22.3	12.2	18.6
upSET	13.0	12.8	19.6	12.3	17.5
CG32152 *	9.1	9.8	19.1	9.6	13.8
CG3527 *	11.2	9.9	16.0	9.1	13.0

282

283 **Figure 2-figure supplement 3. Expression of selected methyltransferases**

284 Expression heat map (bulk RNAseq) of 43 selected Drosophila methyltransferases in circulating
285 hemocytes from uninfected (Uninf) and infected (INF) third instar larvae collected at 0, 9 and 18 hpi (0
286 hpi = 72 hours after egg laying). Means of 6 replicates (10 replicates in case of 18 h INF) shown in each
287 cell are transcripts per million (TPM) - for comparison, only 20% of genes in RNAseq show expression
288 higher than 15 TPM (data in S1_Data and S4_Data). These 43 selected methyltransferases out of 200 (S3
289 Data) all significantly increase expression upon infection at both 9 and 18 h (statistical data in S1 Data).
290 Asterisks after gene names indicate SAM-dependent methyltransferases as categorized in Flybase; some
291 of the unlabeled genes may still belong to SAM-dependent methyltransferases.

292

293 **Ahcy produces adenosine as a systemic signal that influences the immune response**

294 In our previous work, we showed that activated hemocytes release increased amount of adenosine
295 (Bajgar et al. 2015; Bajgar and Dolezal 2018). This causes a systemic metabolic switch that slows the
296 organism's development, leaving energy for an effective immune response. Our results show that the
297 SAM transmethylation pathway is enhanced in hemocytes after infection. This means that increased
298 levels of adenosine is produced, as every methylation event results in the production of one adenosine
299 molecule. At the same time, the cell must rapidly remove adenosine, along with homocysteine, to avoid
300 reversing the direction of Ahcy enzyme activity, which would block methylation. This appears to be
301 reflected in the significant reduction in intracellular adenosine levels after infection (Figure 3A). At least
302 part of this reduction is likely due to the release of adenosine from the cell (via the equilibrative
303 nucleoside transporter ENT2 (Bajgar et al. 2015)) since extracellular adenosine levels increase after
304 infection (Figure 3B), as does the level of inosine, which is formed from adenosine by the action of the
305 adenosine deaminase ADGF-A. We measured the extracellular adenosine production in hemocytes after
306 20 minutes of *ex vivo* incubation, when hemocytes were removed by centrifugation and adenosine and
307 inosine were measured in the collected supernatants. We also chose to detect inosine because activated
308 hemocytes produce the adenosine deaminase ADGF-A (Novakova and Dolezal 2011). Therefore, some
309 adenosine is always converted to inosine during sample processing, even when the adenosine
310 deaminase inhibitor EHNA (erythro-9-(2-hydroxy-3-nonly)adenine) is used, otherwise it is difficult to
311 detect any adenosine.

312 Hemocyte-specific Ahcy RNAi leads to a significant decrease in intracellular adenosine levels, confirming
313 that a significant fraction of adenosine is generated by the SAM transmethylation pathway (Figure 3A).
314 However, there is no increase in extracellular adenosine, or inosine levels upon Ahcy knockdown in
315 hemocytes following infection (Figure 3B). This indicates that the SAM transmethylation pathway is
316 responsible for the generation of this extracellular signal. This is further supported by the fact that
317 silencing of Ahcy in hemocytes during infection leads to a significant reduction (by 6 hours) in
318 developmental delay (Figure 3C), the hallmark of systemic effects of adenosine during infection. Similar
319 to our previous work (Bajgar et al. 2015), this results in diminished host defense, which is associated
320 with reduced production of lamellocytes and encapsulation of the parasitoid (Figure 3D) and reduced
321 survival (Figure 3E). Interestingly, the induction of Ahcy RNAi in hemocytes accelerates development by
322 approximately 2 hours, even in the absence of infection (Figure 3C), a result similar to silencing ENT2
323 specifically in hemocytes (Bajgar et al. 2015). The normal activity of hemocytes, associated with
324 methylation and adenosine release, appears to slow the overall development of the organism.

325 In summary, the SAM transmethylation pathway and Ahcy produce the majority of adenosine in
326 *Drosophila* larval hemocytes and strongly participate in the production of extracellular adenosine as a
327 systemic metabolic regulator. Knockdown of Ahcy in hemocytes reduces larval developmental delay
328 associated with infection, demonstrating the lack in extracellular adenosine production. In addition,
329 knockdown of Ahcy in hemocytes negatively impacts immune response.

330

331

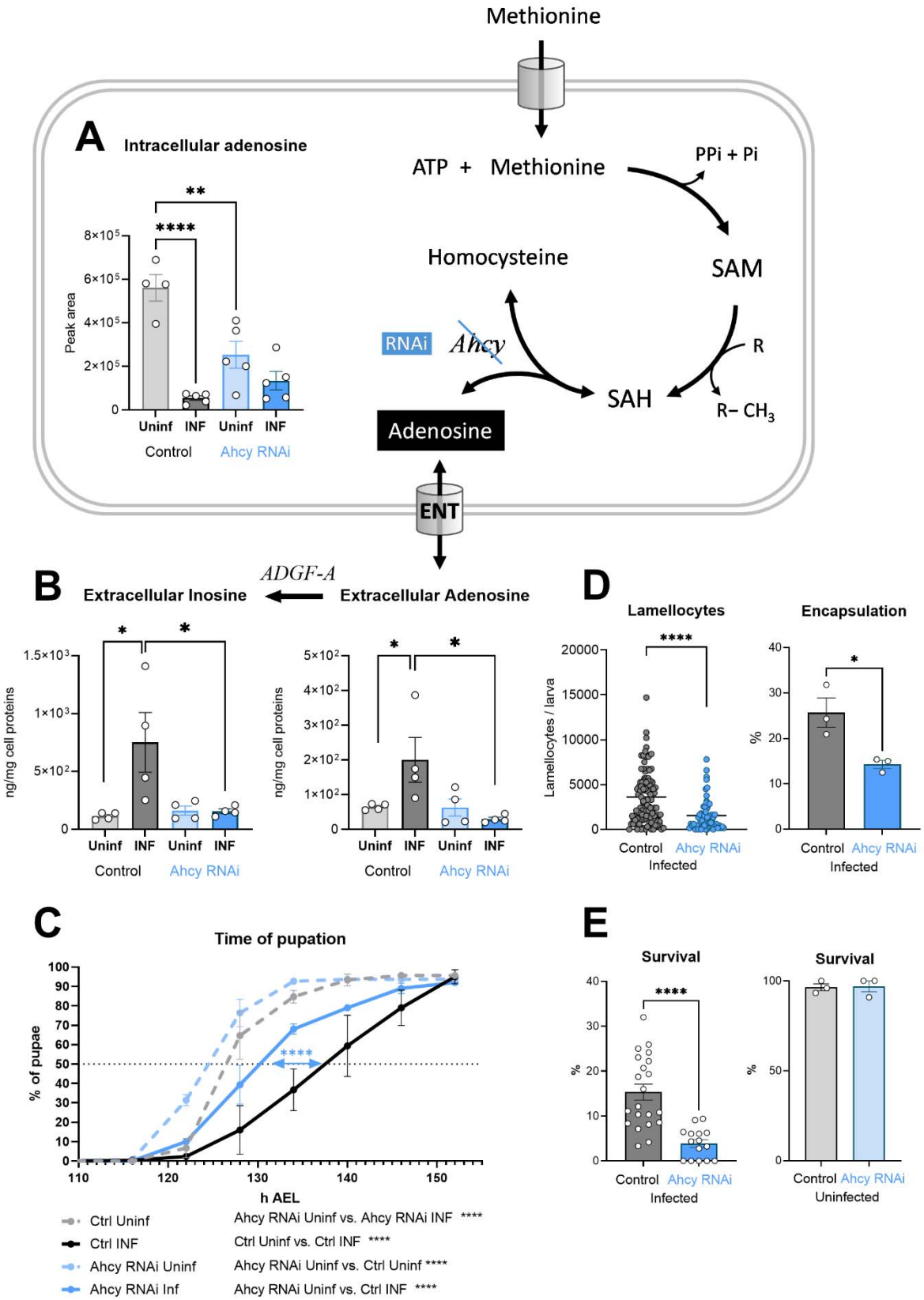
Methionine
A
Intracellular adenosine
ATP + Methionine
PPi + Pi
SAM
Homocysteine
RNAi
Ahcy
R
SAH
R– CH3
Adenosine
ENT
Peak area
Uninf INF Uninf INF
Control Ahcy RNAi
B
Extracellular Inosine
ADGF-A
Extracellular Adenosine
ng/mg cell proteins
C
Time of pupation
% of pupae
h AEL
Ctrl Uninf
Ctrl INF
Ahcy RNAi Uninf
Ahcy RNAi Inf
Ahcy RNAi Uninf vs. Ahcy RNAi INF ****
Ctrl Uninf vs. Ctrl INF ****
Ahcy RNAi Uninf vs. Ctrl Uninf ****
Ahcy RNAi Uninf vs. Ctrl INF ****
D
Lamellocytes
Encapsulation
Lamellocytes / larva
%
Control Ahcy RNAi
Infected
E
Survival
Control Ahcy RNAi
Infected
Uninfected

332

333 **Figure 3. Generation of adenosine in the SAM transmethylation pathway and its systemic effects**

334 (A) Levels of intracellular adenosine in hemocytes shown as the mean metabolite amount expressed by
335 the normalized peak area at 20 hpi. Infection significantly decreases the level in control hemocytes
336 (uninfected - Uninf - light gray vs. infected - INF - dark gray). Hemocyte-specific adenosylhomocysteinase
337 knockdown (Ahcy RNAi; uninfected - Uninf - light blue and infected - INF - dark blue) significantly
338 decreases intracellular adenosine in the uninfected state. (B) Levels of extracellular adenosine (right),
339 released from hemocytes ex vivo after 20 min, and extracellular inosine (left) generated by adenosine
340 deaminase ADGF-A. While infection leads to increased release of adenosine and generated inosine in
341 the control (gray), no such increase is detected with Ahcy RNAi (blue). (C) Pupation is delayed upon
342 infection in control larvae (n = 270, uninfected dashed gray line and n = 240, infected solid black line) but
343 significantly less in hemocyte-specific Ahcy RNAi larvae (n = 260, uninfected dashed blue line and n =
344 265, infected solid blue line). Lines represent percentages of pupae at hours after egg laying (h AEL);
345 rates were compared using Log-rank survival analysis. (D) The number of lamellocytes as well as
346 encapsulation efficiency is significantly lower in infected Ahcy-RNAi (blue) larvae compared to infected
347 control (gray). (E) Percentage of infected larvae surviving to adulthood is significantly lower in Ahcy-RNAi
348 (blue) compared to control (gray) while the survival of uninfected individuals is not affected. (A,B,E) Bars
349 represent means with SEM of uninfected (Uninf, light gray) and infected (INF, dark gray) control and
350 uninfected (Uninf, light blue) and infected (INF, dark blue) Ahcy-RNAi samples; each dot represents a
351 biological replicate; (D) dots represent the number of lamellocytes in a larva and the line mean;
352 numerical values are in S1_Data and S2_data; asterisks represent significant differences between
353 samples tested and unpaired t test (*p<0.05, **p<0.01, ***p<0.001, ****p<0.0001).

354

355 **Activated hemocytes recycle ATP and SAM from adenosine**

356 The above results demonstrate that the SAM transmethylation pathway is a major producer of
357 adenosine in activated hemocytes. To maintain methylation, the cell must rapidly remove adenosine,
358 some of which is released from the cell. This, of course, reduces the adenosyl pool of the cell; note that
359 the SAM pathway is a major consumer of ATP when it combines methionine with ATP to form SAM
360 (Figure 4A). Therefore, activated immune cells have active *de novo* purine production, as shown in
361 mammalian macrophages and T lymphocytes (Yu et al. 2019; Roy et al. 2020). Our recent work showed
362 increased pentose phosphate pathway activity is linked with nucleotide production in activated
363 hemocytes (Kazek et al. 2024). However, this is very energy consuming and requires many steps,
364 whereas the recycling of adenosine to AMP requires only one step and one ATP. Ahcy activity has indeed
365 been linked to adenosine kinase activity, which produces AMP from Ado (Moffatt et al. 2002; Xu et al.
366 2017; Murugan et al. 2021). AMP can then be converted to ADP by adenylate kinase (P. Dzeja and Terzic
367 2009) and finally to ATP by glycolysis or OXPHOS, which can again enter the transmethylation pathway.

368 The most striking expression change we detected in activated hemocytes was the increase of adenosine
369 kinase Adk3 (Figure 4B and C) and cytosolic adenylate kinase Ak1 (Figure 4B and D). Another adenosine
370 kinase, Adk2, which is not altered by infection, is also highly expressed in hemocytes, as is the
371 mitochondrial adenylate kinase Ak2 (Figure 4 B-D). Activated hemocytes have a system for recycling
372 adenosine back to ATP, which appears to be further enhanced during infection. The increase of cytosolic
373 Ak1 indicates at least partial redirection of energy metabolism from mitochondria (oxidative
374 phosphorylation) into cytosol (aerobic glycolysis) in activated immune cells (Kornberg 2020).

375 The increase in all levels of IMP, AMP, ADP and ATP (Figure 4E-H) indicates that *de novo* nucleotide
376 production occurs in activated hemocytes. *De novo* purine synthesis may play many different roles in
377 the cell, but an important one is the replenishment of ATP for SAM synthesis. In addition to *de novo*
378 synthesis, our expression analysis suggests that recycling of adenosine to ATP is also involved. We tested
379 this by adding labeled adenosine to resting and activated hemocytes *ex vivo* (Figure 4A). Since
380 hemocytes express ENT2 (Figure 4B and Bajgar et al. 2015), at least some of the labeled adenosine
381 enters the hemocytes and is converted to AMP and finally to ATP (Figure 4I and J). This demonstrates
382 that hemocytes recycle adenosine to ATP, in addition to *de novo* purine synthesis. Both the AMP m+5
383 and ATP m+5 fractions are lower after infection (Figure 4I and J). This is likely due to dilution of the
384 labeled fraction by a significant increase in newly synthesized, unlabeled AMP and ATP (Figure 4F and
385 H). Activated hemocytes also release more adenosine from the cell, so it is possible that it is more
386 difficult for labeled adenosine to enter the cell. Therefore, the extent of ATP recycling from adenosine in
387 resting and activated hemocytes remains elusive.

388 Resting hemocytes show a diminished fraction of labeled SAM derived from labeled adenosine (Figure
389 4K). After infection, there is a significant increase in SAM labeling (Figure 4K), with approximately 13%
390 of labeled ATP molecules being used for SAM synthesis (compare Figure 4J to Figure 4K), while the total
391 level of SAM does not change (Figure 4L). Since ATP is labeled to greater extent in resting hemocytes,
392 this suggests a compartmentalization of the enzymatic cascade physically linking SAM to adenosine
393 recycling (Pedley and Benkovic 2017; Bar-Peled and Kory 2022). If any ATP was used for SAM
394 production, then a higher fraction of labeled ATP in resting hemocytes should be reflected in higher
395 labeled SAM fractions. A higher fraction of labeled SAM in activated hemocytes suggests a physical
396 connection of SAM synthesis and ATP recycling from labeled adenosine. Increased recycling of
397 adenosine to ATP would be characterized by more 13C entering SAM, despite the fraction of labeled ATP
398 appearing lower due to the total amount of ATP produced by *de novo* synthesis.

399 In conclusion, both resting and activated hemocytes recycle adenosine to ATP. Activated hemocytes
400 strongly upregulate the expression of Adk3 and cytosolic Ak1 and increase production of SAM from
401 recycled adenosine.

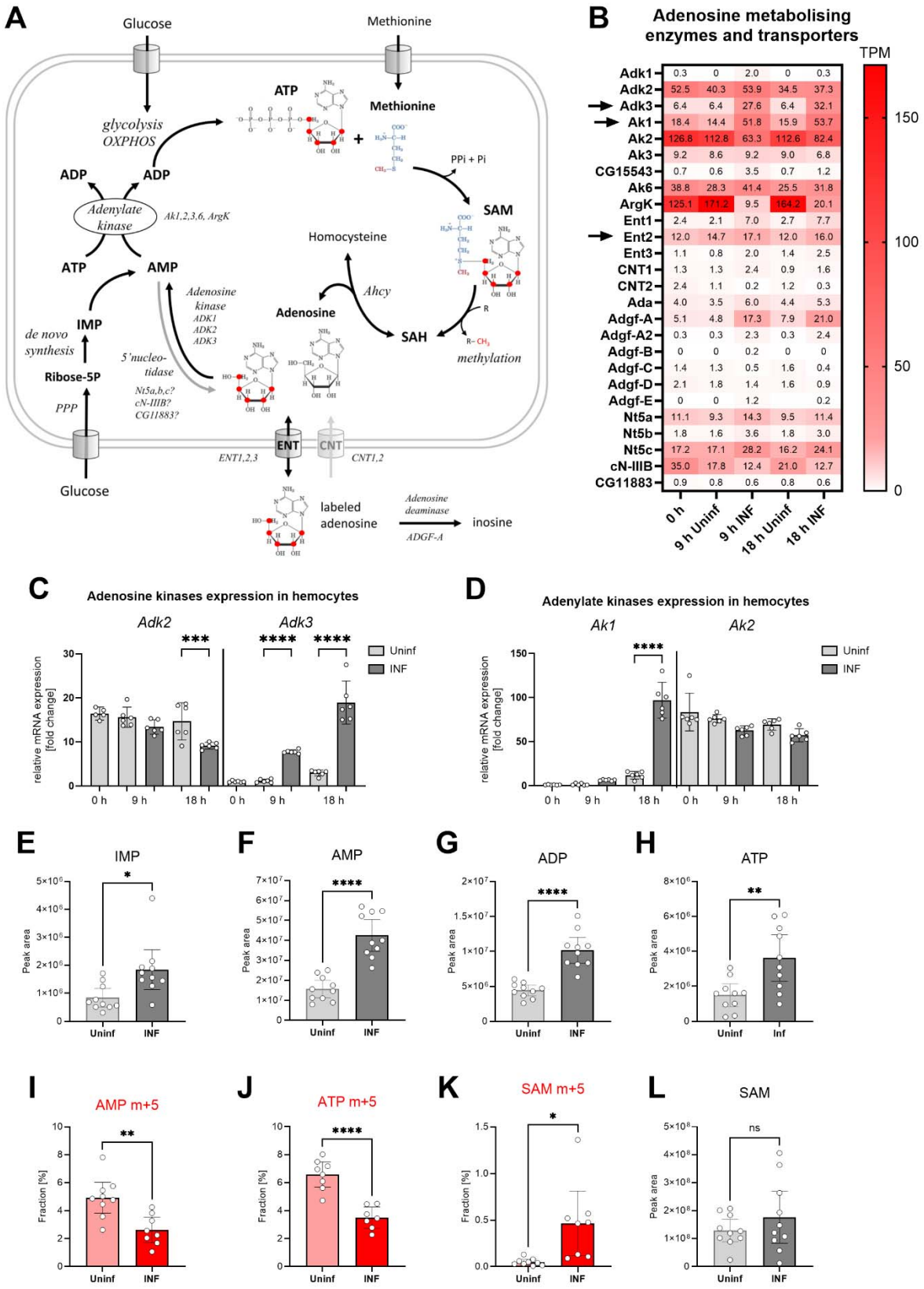
A
Glucose
Methionine
ATP
Methionine
glycolysis
OXPHOS
PPi + Pi
ADP
ADP
SAM
Adenylate kinase
Ak1,2,3,6, ArgK
Homocysteine
ATP
AMP
Adenosine kinase
ADK1
ADK2
ADK3
Ahcy
Adenosine
IMP
de novo synthesis
SAH
methylation
5'nucleo-tidase
Ribose-5P
Nt5a,b,c?
cN-IIIB?
CG11883?
PPP
ENT
CNT
ENT1,2,3
CNT1,2
Glucose
labeled adenosine
Adenosine deaminase
ADGF-A
inosine
B
Adenosine metabolising enzymes and transporters
TPM
Adk1 0.3 0 2.0 0 0.3
Adk2 52.5 40.3 53.9 34.5 37.3
Adk3 6.4 6.4 27.6 6.4 32.1
Ak1 18.4 14.4 51.8 15.9 53.7
Ak2 126.8 112.8 63.3 112.6 82.4
Ak3 9.2 8.6 9.2 9.0 6.8
CG15543 0.7 0.6 3.5 0.7 1.2
Ak6 38.8 28.3 41.4 25.5 31.8
ArgK 125.1 171.2 9.5 164.2 20.1
Ent1 2.4 2.1 7.0 2.7 7.7
Ent2 12.0 14.7 17.1 12.0 16.0
Ent3 1.1 0.8 2.0 1.4 2.5
CNT1 1.3 1.3 2.4 0.9 1.6
CNT2 2.4 1.1 0.2 1.2 0.3
Ada 4.0 3.5 6.0 4.4 5.3
Adgf-A 5.1 4.8 17.3 7.9 21.0
Adgf-A2 0.3 0.3 2.3 0.3 2.4
Adgf-B 0 0 0.2 0 0
Adgf-C 1.4 1.3 0.5 1.6 0.4
Adgf-D 2.1 1.8 1.4 1.6 0.9
Adgf-E 0 0 1.2 0.2
Nt5a 11.1 9.3 14.3 9.5 11.4
Nt5b 1.8 1.6 3.6 1.8 3.0
Nt5c 17.2 17.1 28.2 16.2 24.1
cN-IIIB 35.0 17.8 12.4 21.0 12.7
CG11883 0.9 0.8 0.6 0.8 0.6
0 h
9 h Uninf
9 h INF
18 h Uninf
18 h INF
150
100
50
0
C
Adenosine kinases expression in hemocytes
Adk2
Adk3
relative mRNA expression [fold change]
Uninf
INF
0 h
9 h
18 h
D
Adenylate kinases expression in hemocytes
Ak1
Ak2
E
IMP
F
AMP
G
ADP
H
ATP
Peak area
Uninf
INF
I
AMP m+5
J
ATP m+5
K
SAM m+5
L
SAM
Fraction [%]
ns

402

403 **Figure 4. Analysis of adenosine recycling to SAM in larval hemocytes by *ex vivo* stable ^{13}C isotope**
404 **tracing**

405 (A) Schematic representation of the SAM transmethylation pathway, *de novo* purine synthesis and
406 adenosine recycling to ATP and SAM and labeling with adenosine-$^{13}C_5$ from media (red 13 represents the
407 labeled carbon). Enzymes and processes are italicized. (B) Expression heat map (bulk RNAseq) of
408 adenosine metabolizing enzymes and transporters in circulating hemocytes from uninfected (Uninf) and
409 infected (INF) third instar larvae collected at 0, 9 and 18 hpi (0 hpi = 72 hours after egg laying). Means of
410 6 replicates (10 replicates in case of 18 h INF) shown in each cell are transcripts per million (TPM) - for
411 comparison, only 20% of genes in RNAseq show expression higher than 15 TPM (data in S1_Data and
412 S4_Data). (C, D) Expression analysis of adenosine kinases Adk2, 3 (C) and adenylate kinases Ak1, 2 (D) in
413 circulating hemocytes from uninfected (Uninf) and infected (INF) third instar larvae collected at 0, 9 and
414 18 hpi by RT-qPCR. Bars show fold change compared to 0 h Adk3 samples (expression levels were
415 normalized to *RpL32* expression in each sample), each dot represents a biological replicate. (E-H, L) Total
416 levels of IMP (E), AMP (F), ADP (G), ATP (H) and S-adenosylmethionine - SAM (L) in hemocytes shown as
417 the mean metabolite amounts expressed by the normalized peak area. (I-K) ^{13}C-labeling of metabolites
418 in hemocytes, which were incubated *ex vivo* for 20 min in media containing 10 µM adenosine-$^{13}C_5$. The
419 graphs show the fraction of the compound with five ^{13}C-labeled carbons – AMP m+5 (I), ATP m+5 (J) and
420 SAM m+5 (K). (C-L) Bars represent mean values with 95% CI of uninfected (Uninf, light gray or pink) and
421 infected (INF, dark gray or red) samples; each dot represents a biological replicate (numerical values in
422 S1_Data and S2_data); asterisks represent significant differences between samples tested by tested by
423 ordinary one-way ANOVA Sidak's multiple comparison test (C,D) and unpaired t test (E-L) (*$p<0.05$,
424 **$p<0.01$, ***$p<0.001$, ****$p<0.0001$).
425

426

427 **Adenosine kinase and cytoplasmic adenylate kinase are important for SAM pathway and immune**
428 **response**

429 To determine the importance of adenosine kinase and adenylate kinase, which seem to be necessary for
430 recycling of ATP from adenosine, we again used hemocyte-specific RNAi induced by Srp-Gal4Gal80. Adk3
431 RNAi reduces the infection-induced increase in expression almost 8 times (Figure 5—figure supplement
432 1). Adk3 expression is low in hemocytes of uninfected larvae (Figure 4B and C), thus we did not observe
433 any effect of Adk3 RNAi on the AMP level in uninfected larvae (Figure 5A). However, there is significantly
434 lower level of AMP in hemocytes from the infected larvae (Figure 5A). Adk2 is also strongly expressed
435 both in resting and activated hemocytes (Figure 4C) and that is, most likely, why we still see an infection-
436 induced increase in AMP upon Adk3 RNAi (Figure 5A). This increase is also due to *de novo* purine
437 synthesis. Nevertheless, the increase in AMP in Adk3 RNAi activated hemocytes is significantly smaller
438 than that of controls, indicating that Adk3 activity is important for adenosine conversion to AMP in
439 activated hemocytes. Increase in methylation index is abrogated upon Adk3 RNAi (Figure 5B), showing
440 that Adk3 activity is required for the infection-induced increase in SAM transmethylation pathway. The
441 consequences of Adk3 knockdown phenocopy those of Ahcy knockdown animals, as development is
442 significantly less delayed during infection (Figure 5C) and number of lamellocytes (Figure 5D), as well as
443 survival (Figure 5E) are decreased. We observe similar effects upon cytoplasmic Ak1 knockdown in
444 hemocytes (Figure 5—figure supplement 1), another enzyme upregulated upon infection, which is likely

445 involved in adenosine recycling. The methylation index is abrogated (Figure 5B), development is
446 significantly less delayed during infection (Figure 5F), number of lamellocytes is decreased (Figure 5G)
447 and survival is lower (Figure 5H) upon Ak1 RNAi mediated knockdown. In summary, recycling of
448 adenosine to AMP and potentially to ATP and SAM, using adenosine kinase and cytoplasmic adenylate
449 kinase, appears to be important for activated hemocytes to increase the SAM transmethylation pathway
450 and for effective immune response.

451

452

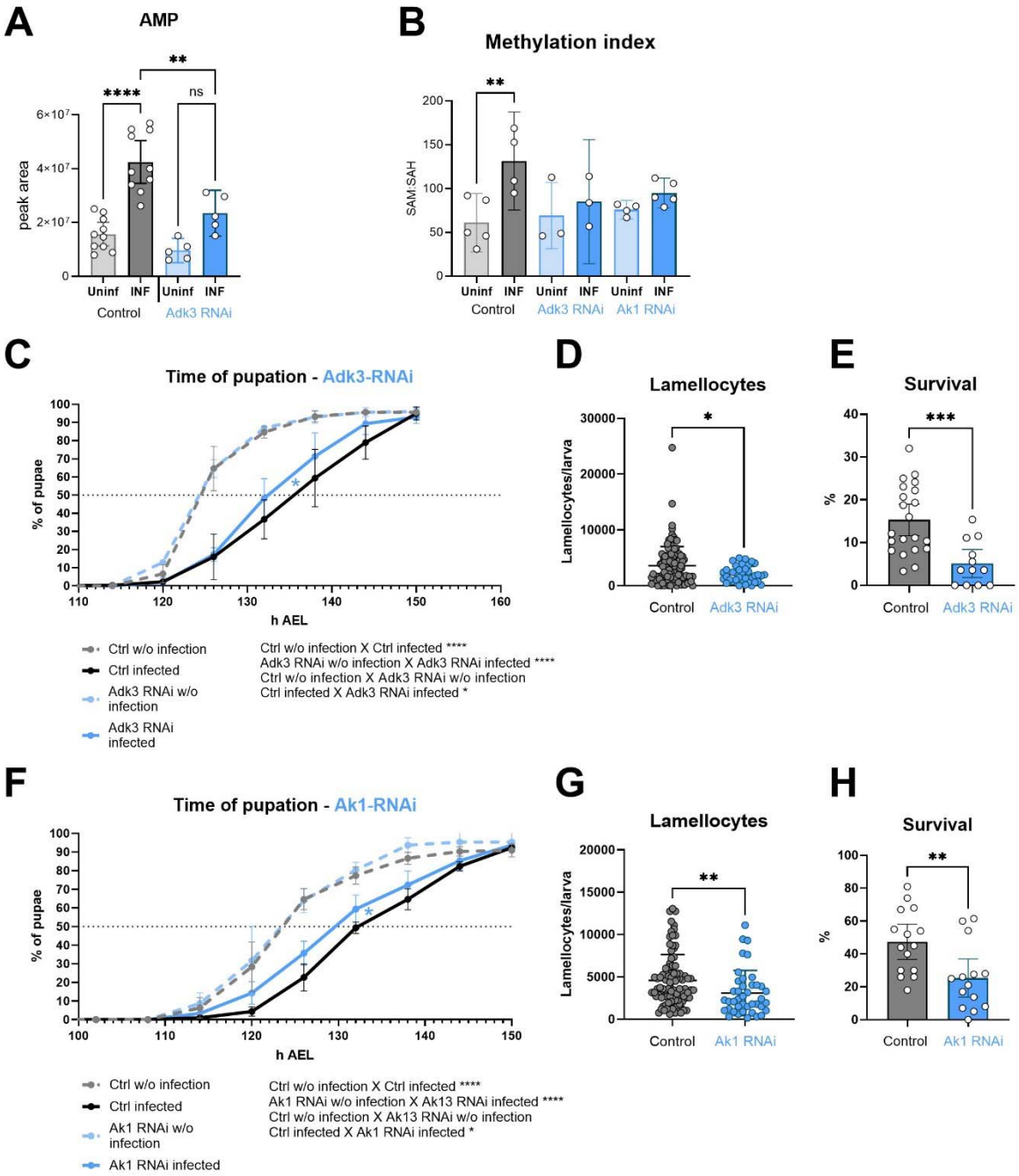

Figure 5. Silencing of adenosine kinase and adenylate kinase in hemocytes affects the SAM transmethylation pathway and immune response

(A) Total levels of AMP in hemocytes shown as the mean metabolite amounts expressed by the normalized peak area. Infection significantly increases the AMP level in control hemocytes (uninfected - Uninf - light gray vs. infected - INF - dark gray). Hemocyte-specific adenosine kinase Adk3 knockdown

460 (Adk3 RNAi; uninfected - Uninf - light blue and infected - INF - dark blue) significantly decreases AMP
461 during infection compared to control. (B) Methylation index, calculated as the ratio of SAM:SAH levels
462 (peak areas; numerical values in S1_Data and S2_data), in control (uninfected - Uninf - light gray and
463 infected - INF - dark gray) and in hemocyte-specific Adk3-RNAi and adenylate kinase Ak1-RNAi
464 (uninfected - Uninf - light blue and infected - INF - dark blue). (C) Pupation is delayed (10 h) upon
465 infection in control larvae (*n* = 270, uninfected dashed gray line and *n* = 240, infected solid black line) but
466 significantly less (7 h) in hemocyte-specific Adk3 RNAi larvae (*n* = 275, uninfected dashed blue line and
467 *n* = 275, infected solid blue line). (D) The number of lamellocytes is significantly lower in infected Adk3-
468 RNAi (blue) larvae compared to infected control (gray). (E) Percentage of infected larvae surviving to
469 adulthood is significantly lower in Adk3-RNAi (blue) compared to control (gray). (F) Pupation is delayed
470 (9 h) upon infection in control larvae (*n* = 225, uninfected dashed gray line and *n* = 270, infected solid
471 black line) but significantly less (6 h) in hemocyte-specific Ak1 RNAi larvae (*n* = 195, uninfected dashed
472 blue line and *n* = 225, infected solid blue line). (G) The number of lamellocytes is significantly lower in
473 infected Ak1-RNAi (blue) larvae compared to infected control (gray). (H) Percentage of infected larvae
474 surviving to adulthood is significantly lower in Ak1-RNAi (blue) compared to control (gray). (A,B,D,E,G,H)
475 Bars/lines represent mean values with 95% CI of uninfected (Uninf, light grey) and infected (INF, dark
476 grey) control and uninfected (Uninf, light blue) and infected (INF, dark blue) Adk3-RNAi or Ak1-RNAi
477 samples; each dot represents one biological replicate (numerical values in S1_Data and S2_data);
478 asterisks represent significant differences between samples tested by unpaired t-test or ordinary one-
479 way ANOVA Tukey's multiple comparison test (*$p<0.05$, **$p<0.01$, ***$p<0.001$, ****$p<0.0001$). (C,F)
480 Lines represent percentages of pupae at hours after egg laying (h AEL); rates were compared using Log-
481 rank survival analysis.

482

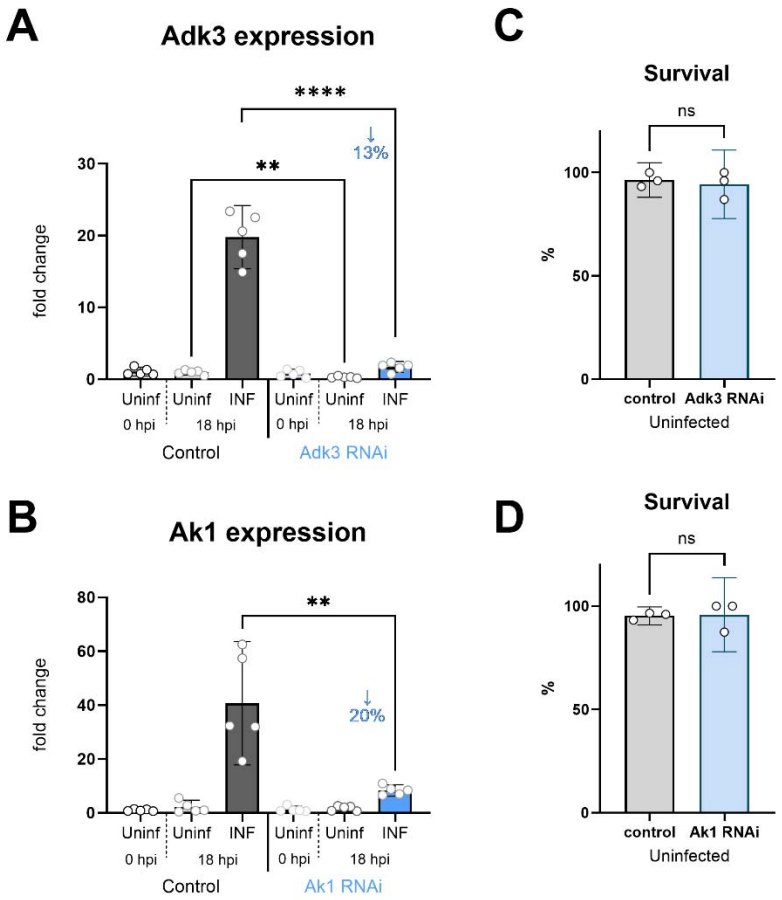

Figure 5-figure supplement 1. Adenosine kinase Adk3 and adenylate kinase Ak1 knockdown efficiency in hemocytes.

Analysis of Adk3 (A) and Ak1 (B) knockdown efficiency at 0 and 18 hpi by RT-qPCR. RNAi was specifically induced in hemocytes by *SrpD-Gal4 tubP-GAL80ts* driven expression of Adk3-RNAi^{HMC06354} or UAS-Ak1-RNAi^{GL00177} in larvae maintained at 18°C for the first 3 days of development and then transferred to 25°C. RNAi reduces Adk3 expression to 13% and Ak1 expression to 20% of control during infection (18 hpi). Bars represent means with 95% CI of uninfected (Uninf, light gray) and infected (INF, dark gray) control (driver crossed to *P{CaryP}Msp300attP40* or *P{CaryP}attP2* control without RNAi) and uninfected (Uninf, light blue) and infected (INF, dark blue) Ahcy-RNAi samples; each dot represents a biological replicate (numerical values in S1_Data); asterisks indicate significant differences between samples tested by ordinary one-way ANOVA Tukey's multiple comparison test (****p<0.0001). Development and survival to adulthood is not affected either by *SrpD-Gal4 tubP-GAL80ts* driven expression of Adk3-RNAi^{HMC06354} (C) or UAS-Ak1-RNAi^{GL00177}(D).

Discussion

We have previously shown that adenosine, released from *Drosophila* hemocytes, is required for systemic metabolic switch and to slow development so that there are enough nutrients for an effective

501 immune response (Bajgar et al. 2015). Here, we show that this signal is generated in hemocytes by the
502 SAM transmethylation pathway, which is enhanced upon infection and is required for the immune
503 response. This novel observation links SAM transmethylation in immune cells to the production of
504 adenosine as a systemic metabolic regulator. In addition, we show that adenosine is not only released
505 from hemocytes but is also recycled to ATP and SAM, mediated by Adk3 and the Ak1, which are
506 necessary for the increase in SAM transmethylation during infection, and therefore effective immune
507 response.

508 The SAM transmethylation pathway is part of the one-carbon metabolism interconnecting the
509 metabolism of serine, glycine, folates, and methionine, supporting *de novo* synthesis of purines and
510 thymidine, and maintaining redox balance. The SAM transmethylation pathway itself controls
511 antioxidant synthesis, sulfur metabolism, polyamine synthesis, and epigenetic programming via
512 methylation (Ducker and Rabinowitz 2017; Vizán, Di Croce, and Aranda 2021). Therefore, Ahcy activity,
513 removing SAH and producing adenosine and homocysteine, is essential, not only for keeping proper
514 function of diverse methyltransferases, but also for a wide range of other essential metabolic processes
515 inside the cell.

516 There is increasing evidence showing the crucial role of the SAM transmethylation pathway in immune
517 cells (Lawson et al. 2012; Klein Geltink and Pearce 2019). It was shown as early as the 80s that peripheral
518 blood mononuclear cells in a "resting" state consume approximately three to five times more SAM for
519 methylation than other, nonhepatic, tissues. Once activated, their SAM consumption is further
520 increased. High SAM utilization was also observed in cultured growing lymphoblasts (German, Bloch,
521 and Kredich 1983). The proper function of the SAM transmethylation pathway and efficient removal of
522 SAH by Ahcy is necessary for chemotaxis in human monocytes, and neutrophils and for lymphocyte
523 effector function (Pike and DeMeester 1988; Zimmerman, Wolberg, and Duncan 1978; Pike, Kredich,
524 and Snyderman 1978). More recently, stable isotope labeling techniques have allowed deeper insight
525 into metabolic set up of activated immune cells. It has been shown that LPS-activated macrophages
526 synergistically increase glycolysis, one carbon metabolism, serine synthesis pathway, pentose phosphate
527 pathway, *de novo* purine synthesis, and SAM transmethylation pathway activity, to induce, and maintain
528 a proinflammatory phenotype. Interestingly, the homocysteine produced by these macrophages is not
529 recycled back into methionine, but SAM synthesis is likely fed exclusively with exogenous methionine
530 transported into the cells (Yu et al. 2019). Roy et al. (2020) demonstrated the metabolic changes that
531 occur in activated CD4+ and CD8+ T lymphocytes. They identified methionine as a crucial metabolite in
532 driving T cells proinflammatory phenotype via epigenetic reprogramming and demonstrated dietary
533 methionine restriction as an effective intervention for autoimmune disease. Activated T lymphocytes,
534 like macrophages, upregulate glycolysis, serine, glycine, and one-carbon metabolism including the SAM
535 transmethylation pathway. These studies indicated that the folate cycle and the SAM transmethylation
536 pathway are uncoupled and homocysteine is not remethylated. Importantly, SAM is synthesized from
537 exogenous methionine and ATP, predominantly produced by *de novo* purine synthesis. Here we show
538 that in *Drosophila* immune cells, SAM is also synthesized mostly from exogenous methionine, and
539 homocysteine is not remethylated back to methionine, but rather used in transsulfuration pathway.
540 Interestingly, our results also suggest an alternative means of CTH production from methionine,
541 independent of Ahcy, although this is not further explored here. Activated hemocytes also increase *de*
542 *novo* purine synthesis, supported by increased pentose phosphate pathway activity (Kazek et al. 2024).

543 Ahcy was shown to play an important role in adenosine production in heart muscle cells, under
544 normoxic conditions (Lloyd et al. 1988; Deussen 1989). Adenosine produced by Ahcy contributes to
545 viability of hepatocellular carcinoma cells (HepG2), since Ahcy knockdown followed by adenosine
546 depletion leads to activation of the DNA damage response, cell cycle arrest, a decreased proliferation
547 rate and DNA damage (Belužić et al. 2018). However, the adenosine formed in the SAM
548 transmethylation pathway is usually referred to in studies as a by-product that needs to be removed
549 quickly to avoid Ahcy reverse function, which would block further methylation. Here, we show that
550 adenosine formed in the SAM transmethylation pathway is not a mere by-product but can have a
551 significant impact on the immune response and the physiology of the whole organism. With the increase
552 of SAM transmethylation pathway activity in activated hemocytes, more adenosine is produced. As
553 intracellularly adenosine decreases, it is released to the extracellular space; this leads to suppression of
554 metabolism in non-immune tissues, and consequently a development delay. This metabolic suppression
555 is crucial for redirecting nutrients towards the immune system and mounting an effective immune
556 response (Bajgar et al. 2015). Knockdown of Ahcy by RNAi suppresses the infection-induced increase in
557 extracellular adenosine, as well as the delay in development, demonstrating that this important
558 systemic signal is most likely generated by the SAM transmethylation pathway. It is important to
559 emphasize that we measured adenosine release only *ex vivo* (short incubation of hemocytes obtained by
560 larval bleeding), because it is extremely challenging to analyze extracellular adenosine levels *in vivo* due
561 to the rapid removal of this molecule. Of course, the *in vivo* situation may be different. We have only
562 been able to detect changes in adenosine levels *in vivo* in a null mutant for the secreted adenosine
563 deaminase ADGF-A (Dolezal et al. 2005) and therefore we rely on genetic manipulations in *in vivo*
564 studies. Using such manipulations, we have shown in previous work that it is activated hemocytes that
565 secrete adenosine as a signal leading to developmental delay (Bajgar et al. 2015). Simply measuring the
566 increase in SAM transmethylation pathway activity in hemocytes, which inevitably leads to increased
567 adenosine production, shows that this pathway at least contributes to the production of this
568 extracellular signal. This is then strongly supported by the phenotypes obtained here using Ahcy-RNAi,
569 which correspond to phenotypes observed after adenosine manipulations (Bajgar et al. 2015).

570 At the same time, we do not want to suggest that SAM transmethylation in hemocytes is the only source
571 of adenosine during infection. Ectoenzymes are an important source of extracellular adenosine that
572 convert extracellular ATP to ADP, AMP and adenosine. This cascade is an important immunomodulator
573 in mammals (Antonioli, Pacher, and Haskó 2022). *Drosophila* also has this cascade of ectoenzymes
574 (Fenckova et al. 2011), which appears not to have an immunomodulatory role, likely due to more
575 rudimentary adenosine signaling (Dolezelova et al., 2007), but could still serve as a source of
576 extracellular adenosine.

577 It is also important to add that while adenosine-mediated metabolic suppression and developmental
578 delay are important for an effective immune response, it is likely that the ineffective immune response
579 in Ahcy RNAi animals is at least in part due to suppression of the SAM transmethylation pathway itself in
580 hemocytes, which is required for their function. Ahcy RNAi not only suppresses the production of
581 adenosine, but also homocysteine, an important precursor for the transsulfuration pathway and thus
582 the production of antioxidants and H_2S; interestingly, our work suggests an alternative production of
583 homocysteine upon Ahcy RNAi. Ahcy RNAi also leads to extensive accumulation of SAH, so we cannot
584 exclude that some phenotypes are due to this accumulation. Even if accumulated SAH would not cause
585 any harm, it suppresses transmethylation reactions and polyamine synthesis, which certainly affects the

586 function of immune cells (Latour, Gobert, and Wilson 2020; Xuan et al. 2023). Therefore, we expect that
587 the effect of Ahcy RNAi on the function of hemocytes is not primarily due to the lack of adenosine as a
588 signal, but rather to the suppression of the SAM transmethylation pathway and its branches.
589 Nevertheless, the increase in the SAM transmethylation pathway in activated hemocytes, leading to
590 increased adenosine production in wild-type hemocytes, and the absence of an increase in extracellular
591 adenosine (at least *ex vivo*) together with the reduced developmental delay (phenotype obtained by
592 manipulating extracellular adenosine by other means) upon hemocyte-specific knockdown of Ahcy
593 strongly suggest the essential role of the SAM transmethylation pathway in generating adenosine as a
594 systemic signal.

595 After ATP, SAM is the most used substrate in the cell, with up to half of the daily methionine intake in
596 humans used for SAM synthesis, the vast majority of which is used for methylation (Lu 2000). If all the
597 adenosine produced by Ahcy was released to hemolymph, hemocytes would likely lose a huge amount
598 of ATP due to SAM synthetase utilizing the adenosyl group of ATP and methionine to create SAM.
599 Increased ATP consumption by the accelerating the SAM transmethylation pathway must be supported
600 by *de novo* purine synthesis. Previous work (Kazek et al. 2024) as well as results presented here, show
601 increased *de novo* purine synthesis in activated immune cells. However, this consumes a considerable
602 amount of energy (6 ATP for one IMP molecule) and takes eleven steps to produce IMP from the initial
603 ribose-5-phosphate. Thus, it is more efficient to recycle at least some ATP from the adenosine generated
604 in the SAM transmethylation pathway via coordinated action of adenosine kinase, cytosolic adenylate
605 kinase, and glycolysis. This is in line with ATP synthesis from adenosine via AMP and ADP shown to be
606 significantly increased in activated rat peritoneal macrophages (Barankiewicz and Cohen 1985).

607 Adenosine kinase has been shown to be coupled with Ahcy to effectively remove adenosine and keep
608 the SAM transmethylation pathway running (Moffatt et al. 2002; Xu et al. 2017; Murugan et al. 2021).
609 Subsequently, the AMP produced can be utilized by the adenylate kinase catalyzing phosphoryl
610 exchange reaction AMP + ATP $\leftrightarrow$ 2 ADP. Adenylate kinase is crucial for cellular energy homeostasis, by
611 regulating nucleotides ratio, AMP production and direction to diverse metabolic sensors (e.g. AMPK). In
612 addition, it is responsible for the transfer of ATP energy rich phosphoryl between energy producing and
613 energy utilizing sites by a sequence of repeated reactions, creating an effective energy transfer shuttle
614 across the cell (R. J. Zeleznikar et al. 1990; Robert J. Zeleznikar, Dzeja, and Goldberg 1995; P. P. Dzeja,
615 Chung, and Terzic 2007; P. Dzeja and Terzic 2009). Our hemocyte RNAseq and qPCR data show that
616 *Drosophila* Adk3 and Ak1 are expressed at low levels in quiescent hemocytes, but their expression
617 increases dramatically during infection. Experiments using 13C labeled adenosine show its incorporation
618 into AMP, ADP, ATP, and especially into SAM, in which the incorporation is significantly increased upon
619 hemocyte activation. These results connect adenosine recycling with the SAM transmethylation
620 pathway. Without infection, the methylation index of Adk3 and Ak1 RNAi in hemocytes is the same as in
621 control cells. However, upon infection, there is no increase in the methylation index in Adk3 and Ak1
622 RNAi cells. When the SAM transmethylation pathway is not accelerated, Ahcy does not produce more
623 adenosine, and consequently the adenosine-induced developmental delay during infection is reduced in
624 Adk3 and Ak1 RNAi, whereas without infection, RNAi larvae develop at the same rate as controls. Our
625 results therefore demonstrate a novel functional connection of adenosine recycling to ATP with SAM
626 transmethylation pathway. At least under energy demanding conditions, as during the activation of
627 immune cells, Adk and cytosolic Ak activities appear to support SAM transmethylation pathway activity.

628 Similar to Ahcy RNAi, Adk3 and Ak1 RNAi in hemocytes also negatively affects immune response
629 efficiency. We see a significant decrease in lamellocytes number in our infected knockdown larvae,
630 resulting in decreased survival. It is important to note, that while Ak1 RNAi most likely also affects *de*
631 *novo* purine synthesis, the Adk3 RNAi effects we observed are due to impairments in adenosine
632 recycling. Connecting the SAM transmethylation pathway-driven production of adenosine with its
633 recycling via Adk3 and Ak1 leads us to following hypothesis (Figure 6):

634 Most cellular processes involve methylation, therefore the SAM transmethylation pathway reflects the
635 activity of the cell. While a wide variety of molecules are methylated, adenosine is the universal product
636 of each individual methylation. Thus, adenosine production reflects the sum of all methylations (where
637 SAM has been used) and therefore the overall activity of the cell. Adenosine must be removed quickly as
638 to not block the SAM transmethylation pathway. The preferred fate is to recycle adenosine to AMP and
639 eventually ATP so that the cell does not lose its adenosyl pool. However, this requires nutrients,
640 adenosine kinase requires ATP, adenylate kinase produces ADP from AMP and ATP and the resulting
641 ADP is recycled to ATP in glycolysis, consuming glucose. If the cell's nutrient supply is inadequate, AMP
642 begins to accumulate, due to the opposite action of adenylate kinase, preventing adenosine from being
643 recycled to AMP by adenosine kinase. In this case, the accumulating adenosine is pushed out of the cell
644 via ENT, where it becomes a signaling molecule, informing surrounding tissues of the need for more
645 nutrients. We therefore look at adenosine as a sensitive sensor of the balance between cell activity
646 (reflected in methylation) and nutrient supply - the better the balance, the less adenosine is released
647 and the more is recycled.

648 To experimentally test this hypothesis will require extremely well controlled conditions, as offered for
649 example by uniform cell culture in precisely controlled media, and delicate manipulation of the
650 important players. The proposed role of adenosine as a sensitive sensor between cell activity and
651 nutrient supply might have far-reaching implications. The production of adenosine by nucleotidase as
652 the ADP/ATP ratio rises is known, for example, to generate a signal in ischemic tissue to inform
653 surrounding tissues of metabolic stress (e.g., vasodilation to increase blood flow). However, the
654 generation of such a signal as a result of an imbalance between cell activity and nutrient supply is a
655 novel and exciting hypothesis.

656 The fate of adenosine is determined by biochemical properties and the expression of enzymes and
657 transporters. The Km values of *Drosophila* Adk2 and Adk3 are not known (Fleischmannova et al. 2012;
658 Stenesen et al. 2013), but it is possible that they differ, and that increased expression of Adk3
659 specifically during infection is important in readjusting the balances between AMP and adenosine, which
660 are determined by the properties of nucleotidases and adenosine kinases (Boison 2013). The expression
661 levels and properties of nucleoside transporters and adenosine deaminase also play important roles.
662 The specific setup of this whole system in certain cell types under certain conditions determines what
663 happens with adenosine (Dulla and Masino 2013; Dale 2021). Studying this setup is essential to
664 understanding the role of this system in specific situations, such as those in which adenosine may be
665 generated by imbalances in activity and energy supply. For example, does it play a role in the early
666 activation of immune cells, regulating nutrient supply to their site of activation? In addition, in the
667 tumor microenvironment, adenosine inhibits infiltrating immune cells (Boison and Yegutkin 2019). Until
668 now adenosine ectoenzymes have been mainly studied in this respect. However, the SAM
669 transmethylation pathway is very active in tumor cells (Vizán, Di Croce, and Aranda 2021) - can tumors
670 regulate their environment by releasing adenosine, which is produced according to our hypothetical

mechanism? Basically, any cell/tissue in which the SAM transmethylation pathway is active can potentially use adenosine as a sensor of the balance between its activity and nutrient supply. Some tissues will probably be more privileged and demand nutrients by releasing adenosine because they have more nucleoside transporters expressed. For example, in the brain, the transmethylation pathway is important for many different processes (Gao 2018), and extracellular adenosine is an important neuromodulator and regulator of blood flow (Peng 2020). Less privileged tissues with lower expression of nucleoside transporters may be more likely to convert adenosine to AMP and activate AMPK during nutrient deprivation to dampen their overactivity. These speculations, of course, need to be tested in the future.

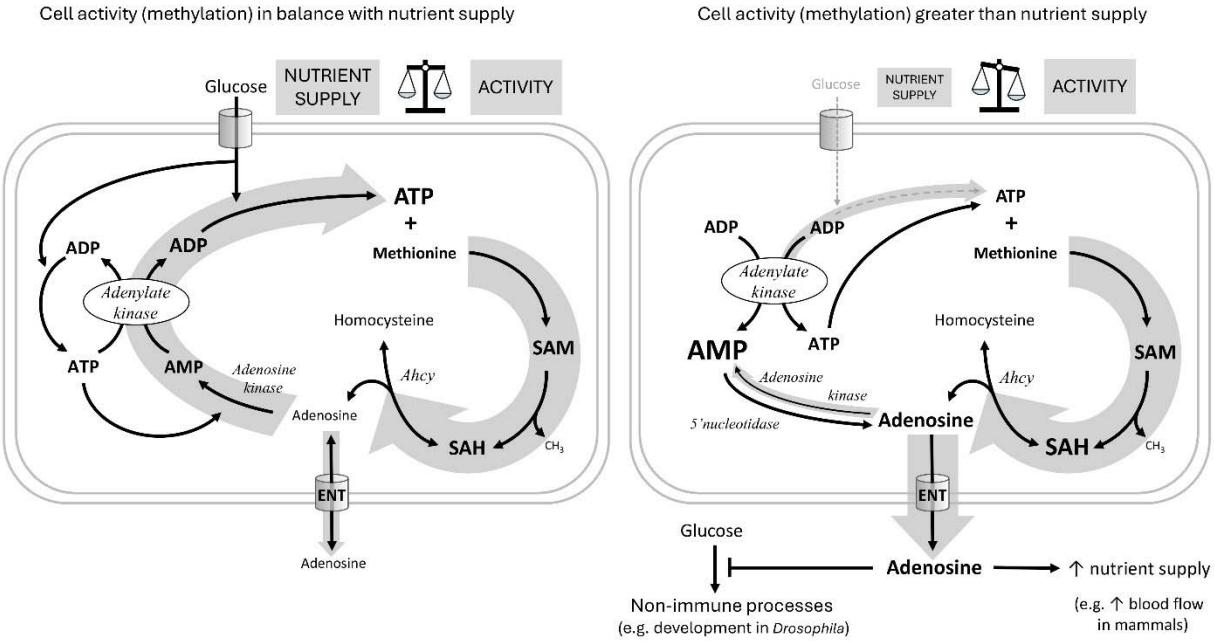

Figure 6. Hypothetical role of adenosine as a sensor of the balance between cell activity and nutrient supply

The hypothetical scheme shows an immune cell with either sufficient (left) or insufficient (right) nutrient supply for the given cellular activity. For each individual transmethylation event using S-adenosylmethionine (SAM) as a methyl group donor and producing S-adenosylhomocysteine (SAH), S-adenosylhomocysteinase (Ahcy) generates one molecule of adenosine (and homocysteine). Adenosine thus reflects the sum of all SAM transmethylations in the cell and may be considered as a proxy for cell activity (thick gray arrow on the right). If there are enough nutrients (cell on the left) to maintain high levels of ATP, adenosine can be recycled first to AMP by adenosine kinase, which requires the first ATP, then to ADP by adenylate kinase, which requires the second ATP, and finally to ATP by glycolysis (or oxidative phosphorylation) using glucose (the gray arrow on the left as thick as the one on the right expresses the balance). Recycled ATP can then enter the next round of transmethylation with methionine to form SAM. If there are not enough nutrients (cell on the right, thin gray arrow on the left)

695 to regenerate ATP from ADP, ATP is produced from two ADP molecules by adenylate kinase,
696 simultaneously generating AMP. Accumulated AMP prevents adenosine recycling by adenosine kinase
697 (thin gray arrow on the left), and on the contrary, more adenosine can be produced from AMP by
698 5'nucleotidase. In this case, adenosine is pushed out of the cell (thick gray arrow down) via the
699 equilibrative nucleoside transporter (ENT) and becomes an extracellular signaling molecule. Extracellular
700 adenosine can, for example, suppress the development of Drosophila larvae or increase blood flow in
701 mammals to provide more nutrients to immune cells.

702

703 **Methods**

704 **Fly strains, cultivation, and parazitoid wasp infection**

705 *Drosophila melanogaster* strain w^{1118} (FBal0018186) in Canton S genetic background (FBst0064349) was
706 used as a control line unless otherwise stated. Strains *UAS-Ahcy-RNAi Ahcy*^{HMS05799} (FBti0186788), UAS-
707 Adk3-RNAi *Adk3*^{HMC06354} (FBti0185498), UAS-Adk2-RNAi *Adk2*^{GL00036} (FBti0144142), UAS-Ak1-RNAi
708 *Ak1*^{GL00177} (FBti0144266), and control lines for RNAi y^1 v^1*; P{CaryP}attP2* (FBst0036303), and y^1 v^1*;*
709 *P{CaryP}Msp300attP40* (FBst0036304) were obtained from the Bloomington Drosophila Stock Center.
710 The *SrpD-Gal4* strain (FBtp0020112) was obtained from M. Crozatier, backcrossed into the w^{1118}
711 background, and recombined with P{tubP-GAL80ts}2 (FBti0027797), which was also backcrossed into
712 w^{1118} background, to generate the w^{1118}; +/+; *SrpD-Gal4* P{tubP-GAL80ts}2 line with Gal4 expression in
713 all hemocytes but not in the fat body when kept at 18°C for the first 3 days of development and then
714 transferred to 25°C (S Fig; expression in the fat body is only present at 29°C in this line). All flies were
715 grown on cornmeal medium (8% cornmeal, 5% glucose, 4% yeast, 1% agar, 0.16% methylparaben) at
716 25°C. Parasitoid wasps *Leptopilina boulardi* were reared on sugar agar medium (6% sucrose, 1.5% agar,
717 0.75% methylparaben) and grown by infection of wild-type *Drosophila* larvae. Early third instar larvae
718 (72 hours after egg laying) were infected with parasitoid wasps (= time point 0 hours). Weak infection
719 (1-2 eggs per larva) was used for survival analysis. Strong infection (4-8 eggs per larva) was used for the
720 rest of the experiments to obtain a strong and more uniform immune response. Infections were
721 performed on 60-mm Petri dishes with standard cornmeal medium for 15 minutes for weak infection
722 and 45 minutes for strong infection.

723

724 **Hemocyte counting**

725 *Drosophila* circulating hemocytes were counted at 20 hpi by bleeding one larva in 15 µL of PBS and using
726 Neubauer hemocytometer (*Brand GMBH*) using differential interference contrast microscopy. Particular
727 types of hemocytes were determined based on the cell morphology and since we were mainly
728 interested in lamellocytes, we counted them 22-24 hours after infection, when most of the lamellocytes
729 from the first wave are fully differentiated but still mostly in circulation, as they are just starting to
730 adhere to the wasp egg.

731

732 **Survival and developmental time analysis**

733 Infected and non-infected 3rd instar larvae were placed into fresh vials in a number of 30 larvae per vial,
734 3 vials per genotype with 3 to 5 independent experiments. Differences in larval development were
735 determined by counting newly appeared pupae every 6 hours post infection. Percentage of pupae
736 number per total used larvae number at particular time points was plotted and compared by Log-rank
737 test. For survival, all emerged adult flies were counted and checked if they contain the melanized eggs
738 to confirm they were infected. The ones without any egg were excluded from the analysis. Percentage of
739 emerged adults number per total used infected individuals were plotted.

740

741 **Gene expression analysis**

742 Based on the larval stage, 30 to 50 larvae were washed 3x in PBS, transferred on microscope slide
743 covered with parafilm and placed on ice. All larvae were opened with tweezers and released
744 hemolymph with hemocytes were aspired with 10 µL pipette and transferred into 1.5 mL tube
745 containing TRIzol Reagent (*Life Technologies*) for RNA extraction. RNA was purified with Direct-zol RNA
746 Microprep (*Zymo-Research*). Total RNA was used for cDNA preparation by PrimeScript Revrese
747 Transcriptase (*Takara*) with oligo(dT) primer. cDNA was used as a template for qPCR using TP SYBR 2x
748 Master Mix (*Top-Bio*) and C1000 Touch Thermal Cycler (*Bio-Rad*). Expression of a specific gene in each
749 sample was normalized to expression of *RpL32* (FBgn0002626) and relative gene expression was
750 counted with ΔΔCt method. Graphs showing target gene expression and statistical analysis were made
751 with GraphPad Prism.

752

753 Primers:

Ahcy	Fw	AAGCTGTCGCACAAATGGCG
	Rev	GCACGTTGTGCACCAGGAAC
AhcyL1	Fw	GGCGAGACGGAAGAGGACT
	Rev	AGAGAGCTGATAGAGACGGTG
Adk2	Fw	AACTTCACCATCGATCACCTGG
	Rev	TAGGAACGGTCGCTGTTTGG
Adk3	Fw	CTGGACATGGAGAAACTCAACC
	Rev	AAAGAAGAGCGCGTCTGTGC
Ak1	Fw	CTCGGCATTGATCGTAAGGG
	Rev	CGATCTGGCGCTGTACTTTG
Ak2	Fw	GCTGAGAAGCTCGACACATTG
	Rev	CTCCAGTGACATCGTCCGTC

Ak3	Fw	GATCCAGCGATTCTTGACCC
	Rev	CGGATAACCGAGGTAGGCAAC
ArgK	Fw	ATGGAGATGATGCGGAGATG
	Rev	TCGACGACCACTTCCTGTTC
Cbs	Fw	AGATTACGCCCAACATCCTCG
	Rev	AATGCGGTCCTTCACTGATCC
CG10621	Fw	CATCGAGCTGATAAAGAACACGG
	Rev	AATGGAGGCAATGATCAAAGGG
CG20623	Fw	ATGCCAAATTCTGGGTCTCCC
	Rev	AAAGGGGTCACGAATAGTGGG
RpL32	Fw	AAGCTGTCGCACAAATGGCG
	Rev	GCACGTTGTGCACCAGGAAC
SamDC	Fw	CAACGGTGACGATGATCTGC
	Rev	AGTTTTAAGGATCCATCGTCGC
SamS	Fw	CAAATCAGCGACGCTATCTTGG
	Rev	TGTCTCACGAACAACCTTCTGG

Bulk RNAseq analysis

RNA was extracted from circulating hemocytes (72 hours after egg laying = time of infection = 0 hours, 81 hours after egg laying = 9 hours post infection/hpi and 90 hours after egg laying = 18 hpi) of uninfected and infected 3rd instar w^{1118} larvae (6-10 replicates) and barcoded 3'-end seq forward libraries were sequenced by deep uni-directional sequencing of 75-base long reads using Illumina NextSeq as described in details in (Kazek et al. 2024). Raw data are available at The European Nucleotide Archive under study accession number: PRJEB74490 (secondary acc: ERP159178) (https://www.ebi.ac.uk/ena/browser/view/PRJEB74490). Trimmed reads were mapped to the BDGP *Drosophila melanogaster* Release 6.29 genomic sequence using the Mapper for RNA Seq in Geneious prime software (Biomatters). Normalized counts of reads mapped to each gene annotation were calculated as transcripts per million (TPM), expression levels were compared using the DESeq2 method in Geneious prime software, and data were exported to an Excel file (S4 Data).

Metabolomics and stable 13C isotope tracing in hemocytes ex vivo

769 Samples for metabolomics were collected 20 hours post infection. Larvae were washed first with
770 distilled water and then with PBS to reduce contamination. Larval hemolymph was collected by carefully
771 tearing the larvae on a glass microscope slide covered with parafilm. Hemolymph from 100 larvae was
772 immediately collected into sterile 1.5 ml Eppendorf polypropylene centrifuge tubes prefilled with 100 µl
773 PBS and centrifuged for 5 min at 25°C, 360xg. For experiments without 13C isotope tracing, hemocytes
774 were resuspended in 50 µL of HPLC water and three times frozen in liquid nitrogen/thawed at 37 °C
775 (established for sufficient cell disruption and extraction of intracellular metabolites). 200 µl of cold
776 acetonitrile-methanol (1:1) was added and stored at -80 °C until LC-HRMS analysis described in Kazek et
777 al. 2024. For experiments with 13C isotope tracing, the supernatant was removed and the cells were
778 mixed with medium containing PBS, 5 mM trehalose, 0.5 mM glucose, 5 mM proline, 5 mM glutamine
779 (*Sigma/MERCK*), supplemented with gentamicin (10 mg/ml; *Gibco*), amphotericin B (250 µg/ml; *Gibco*)
780 and 0.1 mM phenylthiourea (PTU; *Sigma/MERCK*) to prevent melanization. Based on the experiment,
781 medium further contained either 0,33 µM L-methionine-$^{13}C_5$ or 10 µM adenosine-$^{13}C_5$ and unlabeled
782 0,33 µM L-methionine. The concentrations are based on measurements of actual hemolymph
783 concentrations in wild-type larvae in the case of methionine, and in the case of adenosine, we used a
784 slightly higher concentration than measured in the *adgf-a* mutant (Dolezal et al. 2005) to have a
785 sufficiently high concentration to allow adenosine to flow into the hemocytes.

786 The hemocytes were then incubated *ex vivo* for 20 min at 25°C and 80-90% humidity. The cells were
787 then centrifuged for 5 min at 25°C, 360xg, the supernatant was removed, the cells were mixed with 50
788 µl of cold PBS and frozen in liquid nitrogen/thawed at 37°C three times (to disrupt the rigid hemocyte
789 cells). Finally, 200 µl of cold acetonitrile-methanol (1:1) was added, in addition, the internal standard 4-
790 fluorophenylalanine (50 ng/sample) was added to control the extraction efficiency and mass
791 spectrometer responses and samples were stored at -80°C until LC-HRMS analysis which is described in
792 Kazek et al. 2024. When extracellular adenosine and inosine were measured, samples were collected in
793 room temperature and centrifuged in 25°C, 5 min, 360xg to wash hemocytes from hemolymph and
794 extracellular metabolites. Cells were resuspended in medium composed of PBS, 5 mM trehalose, 0.5
795 mM glucose, 5 mM proline, 5 mM glutamine, 0.33 mM methionine (*Sigma/MERCK*), supplemented with
796 gentamicin (10 mg/ml; *Gibco*), amphotericin B (250 µg/ml; *Gibco*), 0.15 mM EHNA (*Sigma/MERCK*) and
797 0.1 mM phenylthiourea (PTU; *Sigma/MERCK*) to prevent melanization. Samples were incubated for 20
798 minutes in room temperature, and then centrifuged in 4°C, 5 min, 360xg. 70 µL of supernatant were
799 transferred into new sterile 1.5 mL Eppendorf polypropylene centrifuge tube containing 70 µL of
800 acetonitrile and stored at -80 °C until LC-HRMS analysis. Pelleted cells were stored in -80°C for protein
801 measurement with QuantiPro™ BCA Assay Kit (*Sigma/MERCK*).

802 Raw data are available at https://doi.org/10.6084/m9.figshare.27291300.v1 and processed data in
803 S2_Data. For peak area analysis, the data were normalized to the total content of all screened unlabeled
804 metabolites - the peak area of the metabolite in a particular sample was divided by the peak area of the
805 same metabolite of the selected reference sample and this procedure was repeated for each individual
806 unlabeled metabolite. These ratios of all metabolites in one particular sample were averaged to
807 determine a normalization factor. We then divided the measured peak area by the normalization factor
808 for that sample to obtain the normalized peak area values (normalization factors are reported in
809 S2_Data).

810

Data analysis

Data were analyzed and graphed using GraphPad Prism (*GraphPad Software*), with specific statistical tests shown in the legend of each figure.

Acknowledgments

The authors acknowledge funding from the Grant Agency of the Czech Republic to TD (Projects 17-16406S and 20-09103S; www.gacr.cz) and from the Grant Agency of the University of South Bohemia in České Budějovice to PN (087/2019/P). We thank Dr. Michele Crozatier and Bloomington Drosophila Stock Center for fly and wasp stocks. We thank Dr. Michalina Kazek for help with metabolomics optimization, to Lucie Hrádková for laboratory management and Marcela Jungwirthová for project management, and all members of Doležal and Moos laboratories for their help with work. We thank Dr. Adam Bajgar for help with bulk RNAseq and Dr. Vladimír Beneš and Genomics Core Facility (EMBL Heidelberg, Germany) for RNAseq services and Dr. Bajgar and Dr. Gabriela Krejčová for help with optimization of the molecular biology methods and wasp infections and general manipulation with flies and larvae. We thank Dr. Ellen McMullen for manuscript editing.

Additional files

S1 Data. Raw data/numerical values for data presented in graphs.

The MS Excel file containing the data used to generate the plots in Figure 2, 3, 4, 5 and Figure 2-figure supplement 1, Figure 2-figure supplement 3 and Figure 5-figure supplement 1. The data for each figure are shown on individual sheets of this file with the panel number indicated next to the data.

S2 Data. Metabolomics and stable ^{13}C isotope tracing in circulating hemocytes during parasitoid wasp infection.

MS Excel sheets with stable ^{13}C isotope tracing experiments. List of metabolites, their characterizations, identification, HPLC/HRMS parameters is on the first sheet [List of Metabolites]. Data from the following experiments are in individual sheets (values are raw or normalized areas under respective chromatographic peaks): [S1] Peak area of metabolites of interest for control and Ahcy RNAi hemocytes. [S2] – Combination of quantitative analysis (ng/sample) and peak area of metabolites of interest for control and Ahcy RNAi hemocytes incubated with 13C5 methionine. [S3] Peak area of metabolites of interest for control and Adk3 RNAi and Ak1 RNAi. [S4] Combination of quantitative analysis (ng/sample) and peak area of metabolites of interest for control and Adk3 RNAi and Ak1 RNAi hemocytes incubated with 13C5 adenosine. Raw data are available at figshare (https://doi.org/10.6084/m9.figshare.27291300.v1).

S3 Data. Methyltransferases gene expression analysis by bulk RNAseq of circulating hemocytes.

MS Excel sheets with expression of genes selected from S4 Data, representing methyltransferases according to Flybase database.

849

850 **S4 Data. Gene expression analysis by bulk RNAseq of circulating hemocytes.**

851 MS Excel sheets with gene expression in circulating hemocytes. RNA was extracted 72 hours after egg
852 laying = time of infection = 0 hours, 81 hours after egg laying = 9 hours post infection/hpi and 90 hours
853 after egg laying = 18 hpi), from hemocytes of the third instar w^{1118} larvae. This table was published in
854 Kazek et al. (2024). Raw data are available at The European Nucleotide Archive under Study accession
855 number: PRJEB74490 (secondary acc: ERP159178)
856 (https://www.ebi.ac.uk/ena/browser/view/PRJEB74490).
857

858 REFERENCES
859

860 Antonioli, Luca, Pál Pacher, and György Haskó. 2022. “Adenosine and Inflammation: It’s Time to
861 (Re)Solve the Problem.” *Trends in Pharmacological Sciences* 43 (1): 43–55.
862 https://doi.org/10.1016/j.tips.2021.10.010.
863 Bajgar, Adam, and Tomas Dolezal. 2018. “Extracellular Adenosine Modulates Host-Pathogen Interactions
864 through Regulation of Systemic Metabolism during Immune Response in Drosophila.” Edited by
865 Brian P. Lazzaro. *PLOS Pathogens* 14 (4): e1007022.
866 https://doi.org/10.1371/journal.ppat.1007022.
867 Bajgar, Adam, Katerina Kucerova, Lucie Jonatova, Ales Tomcala, Ivana Schneedorferova, Jan Okrouhlik,
868 and Tomas Dolezal. 2015. “Extracellular Adenosine Mediates a Systemic Metabolic Switch during
869 Immune Response.” Edited by Marc S. Dionne. *PLOS Biology* 13 (4): e1002135.
870 https://doi.org/10.1371/journal.pbio.1002135.
871 Barankiewicz, Jerzy, and Amos Cohen. 1985. “Purine Nucleotide Metabolism in Resident and Activated
872 Rat Macrophages *in Vitro*.” *European Journal of Immunology* 15 (6): 627–31.
873 https://doi.org/10.1002/eji.1830150618.
874 Bar-Peled, Liron, and Nora Kory. 2022. “Principles and Functions of Metabolic Compartmentalization.”
875 *Nature Metabolism* 4 (10): 1232–44. https://doi.org/10.1038/s42255-022-00645-2.
876 Belužić, Lucija, Ivana Grbeša, Robert Belužić, Jong Hoon Park, Hyun Kyung Kong, Nevenka Kopjar,
877 Guadalupe Espadas, et al. 2018. “Knock-down of AHCY and Depletion of Adenosine Induces DNA
878 Damage and Cell Cycle Arrest.” *Scientific Reports* 8 (1): 14012. https://doi.org/10.1038/s41598-
879 018-32356-8.
880 Bjursell, Magnus K., Henk J. Blom, Jordi Asin Cayuela, Martin L. Engvall, Nicole Lesko, Shanti
881 Balasubramaniam, Göran Brandberg, et al. 2011. “Adenosine Kinase Deficiency Disrupts the
882 Methionine Cycle and Causes Hypermethioninemia, Encephalopathy, and Abnormal Liver
883 Function.” *The American Journal of Human Genetics* 89 (4): 507–15.
884 https://doi.org/10.1016/j.ajhg.2011.09.004.
885 Boison, Detlev. 2013. “Adenosine Kinase: Exploitation for Therapeutic Gain.” Edited by Stephen P.H.
886 Alexander. *Pharmacological Reviews* 65 (3): 906–43. https://doi.org/10.1124/pr.112.006361.
887 Boison, Detlev, and Michael F. Jarvis. 2021. “Adenosine Kinase: A Key Regulator of Purinergic
888 Physiology.” *Biochemical Pharmacology* 187 (May):114321.
889 https://doi.org/10.1016/j.bcp.2020.114321.
890 Boison, Detlev, and Gennady G. Yegutkin. 2019. “Adenosine Metabolism: Emerging Concepts for Cancer
891 Therapy.” *Cancer Cell* 36 (6): 582–96. https://doi.org/10.1016/j.ccell.2019.10.007.
892 Dale, Nicholas. 2021. “Biological Insights from the Direct Measurement of Purine Release.” *Biochemical*
893 *Pharmacology* 187 (May):114416. https://doi.org/10.1016/j.bcp.2021.114416.
894 Deussen, A. 1989. “Contribution of S-Adenosylhomocysteine to Cardiac Adenosine Formation.” *Journal*
895 *of Molecular and Cellular Cardiology* 21 (8): 773–82. https://doi.org/10.1016/0022-
896 2828(89)90716-5.
897 Dilek, Nahzli, Andreas Papapetropoulos, Tracy Toliver-Kinsky, and Csaba Szabo. 2020. “Hydrogen Sulfide:
898 An Endogenous Regulator of the Immune System.” *Pharmacological Research* 161
899 (November):105119. https://doi.org/10.1016/j.phrs.2020.105119.
900 Dolezal, Tomas. 2015. “Adenosine: A Selfish-Immunity Signal?” *Oncotarget* 6 (32): 32307–8.
901 https://doi.org/10.18632/oncotarget.4685.
902 Dolezal Tomas, Dolezelova Eva, Zurovec Michal, Peter J. Bryant. 2005. "A Role for Adenosine Deaminase
903 in Drosophila Larval Development.". *PLoS Biol* 3 (7): e201.
904 https://doi.org/10.1371/journal.pbio.0030201

Dolezelova, Eva, Hans-Peter Nothacker, Olivier Civelli, Peter J. Bryant, and Michal Zurovec. 2007. “A Drosophila Adenosine Receptor Activates cAMP and Calcium Signaling.” *Insect Biochemistry and Molecular Biology* 37 (4): 318–29. https://doi.org/10.1016/j.ibmb.2006.12.003.

Ducker, Gregory S., and Joshua D. Rabinowitz. 2017. “One-Carbon Metabolism in Health and Disease.” *Cell Metabolism* 25 (1): 27–42. https://doi.org/10.1016/j.cmet.2016.08.009.

Dulla, Chris G., and Susan A. Masino. 2013. “Physiologic and Metabolic Regulation of Adenosine: Mechanisms.” In *Adenosine*, edited by Susan Masino and Detlev Boison, 87–107. New York, NY: Springer New York. https://doi.org/10.1007/978-1-4614-3903-5_5.

Dzeja, Petras P., Susan Chung, and Andre Terzic. 2007. “Integration of Adenylate Kinase and Glycolytic and Glycogenolytic Circuits in Cellular Energetics.” In *Molecular System Bioenergetics*, edited by Valdur Saks, 1st ed., 265–301. Wiley. https://doi.org/10.1002/9783527621095.ch8.

Dzeja, Petras, and Andre Terzic. 2009. “Adenylate Kinase and AMP Signaling Networks: Metabolic Monitoring, Signal Communication and Body Energy Sensing.” *International Journal of Molecular Sciences* 10 (4): 1729–72. https://doi.org/10.3390/ijms10041729.

Fenckova, Michaela, Radka Hobizalova, Zdenek Faltynek Fric, and Tomas Dolezal. 2011. “Functional Characterization of Ecto-5′-Nucleotidases and Apyrases in Drosophila Melanogaster.” *Insect Biochemistry and Molecular Biology* 41 (12): 956–67. https://doi.org/10.1016/j.ibmb.2011.09.005.

Fleischmannova, Jana, Lucie Kucerova, Katerina Sandova, Veronika Steinbauerova, Vaclav Broz, Petr Simek, and Michal Zurovec. 2012. “Differential Response of Drosophila Cell Lines to Extracellular Adenosine.” *Insect Biochemistry and Molecular Biology* 42 (5): 321–31. https://doi.org/10.1016/j.ibmb.2012.01.002.

Fredholm, Bertil B., Stina Johansson, and Ying-Qing Wang. 2011. “Adenosine and the Regulation of Metabolism and Body Temperature.” In *Advances in Pharmacology*, 61:77–94. Elsevier. https://doi.org/10.1016/B978-0-12-385526-8.00003-5.

Gao Jin, Cahill Catherine M., Huang Xudong, Roffman Joshua L., Lamon-Fava Stefania, Fava Maurizio, Mischoulon David & Rogers Jack T.. 2018. "S-Adenosyl Methionine and Transmethylation Pathways in Neuropsychiatric Diseases Throughout Life." *Neurotherapeutics, 15(1), 156–175.* doi:10.1007/s13311-017-0593-010.1007/s13311-017-0593-0

German, D. C., C. A. Bloch, and N. M. Kredich. 1983. “Measurements of S-Adenosylmethionine and L-Homocysteine Metabolism in Cultured Human Lymphoid Cells.” *The Journal of Biological Chemistry* 258 (18): 10997–3.

Kazek, Michalina, Lenka Chodáková, Katharina Lehr, Lukáš Strych, Pavla Nedbalová, Ellen McMullen, Adam Bajgar, et al. 2024. “Glucose and Trehalose Metabolism through the Cyclic Pentose Phosphate Pathway Shapes Pathogen Resistance and Host Protection in Drosophila.” Edited by Alex P. Gould. *PLOS Biology* 22 (5): e3002299. https://doi.org/10.1371/journal.pbio.3002299.

Klein Geltink, Ramon I, and Erika L Pearce. 2019. “The Importance of Methionine Metabolism.” *eLife* 8 (May):e47221. https://doi.org/10.7554/eLife.47221.

Kloor, Doris, and Hartmut Osswald. 2004. “S-Adenosylhomocysteine Hydrolase as a Target for Intracellular Adenosine Action.” *Trends in Pharmacological Sciences* 25 (6): 294–97. https://doi.org/10.1016/j.tips.2004.04.004.

Kornberg, Michael D. 2020. “The Immunologic Warburg Effect: Evidence and Therapeutic Opportunities in Autoimmunity.” *WIREs Systems Biology and Medicine* 12 (5): e1486. https://doi.org/10.1002/wsbm.1486.

Krejčová, Gabriela, Cecilia Morgantini, Helena Zemanová, Volker M Lauschke, Julie Kovářová, Jiří Kubásek, Pavla Nedbalová, et al. 2023. “Macrophage-derived Insulin Antagonist *ImpL2* Induces

952 Lipoprotein Mobilization upon Bacterial Infection." *The EMBO Journal* 42 (23): e114086.
953 https://doi.org/10.15252/embj.2023114086.
954 Kroll, K, A Deussen, and I R Sweet. 1992. "Comprehensive Model of Transport and Metabolism of
955 Adenosine and S-Adenosylhomocysteine in the Guinea Pig Heart." *Circulation Research* 71 (3):
956 590–604. https://doi.org/10.1161/01.RES.71.3.590.
957 Latour, Yvonne L., Alain P. Gobert, and Keith T. Wilson. 2020. "The Role of Polyamines in the Regulation
958 of Macrophage Polarization and Function." *Amino Acids* 52 (2): 151–60.
959 https://doi.org/10.1007/s00726-019-02719-0.
960 Lawson, Brian R., Theodoros Eleftheriadis, Virginie Tardif, Rosana Gonzalez-Quintial, Roberto Baccala,
961 Dwight H. Kono, and Argyrios N. Theofilopoulos. 2012. "Transmethylation in Immunity and
962 Autoimmunity." *Clinical Immunology* 143 (1): 8–21. https://doi.org/10.1016/j.clim.2011.10.007.
963 Lecoq, K., I. Belloc, C. Desgranges, and B. Daignan-Fornier. 2001. "Role of Adenosine Kinase in
964 Saccharomyces Cerevisiae: Identification of the ADO1 Gene and Study of the Mutant
965 Phenotypes." *Yeast* 18 (4): 335–42. https://doi.org/10.1002/1097-
966 0061(20010315)18:4<335::AID-YEA674>3.0.CO;2-X.
967 Lloyd, H G, A Deussen, H Wuppermann, and J Schrader. 1988. "The Transmethylation Pathway as a
968 Source for Adenosine in the Isolated Guinea-Pig Heart." *Biochemical Journal* 252 (2): 489–94.
969 https://doi.org/10.1042/bj2520489.
970 Lu, Shelly C. 2000. "S-Adenosylmethionine." *The International Journal of Biochemistry & Cell Biology* 32
971 (4): 391–95. https://doi.org/10.1016/S1357-2725(99)00139-9.
972 McMullen, Ellen, Lukas Strych, Lenka Chodakova, Amber Krebs, and Tomas Dolezal. 2024. "JAK/STAT
973 Mediated Insulin Resistance in Muscles Is Essential for Effective Immune Response." *Cell
974 Communication and Signaling* 22 (1): 203. https://doi.org/10.1186/s12964-024-01575-0.
975 Moffatt, Barbara A., Yvonne Y. Stevens, Michael S. Allen, Jamie D. Snider, Luiz A. Pereira, Margarita I.
976 Todorova, Peter S. Summers, Elizabeth A. Weretilnyk, Luke Martin-McCaffrey, and Conrad
977 Wagner. 2002. "Adenosine Kinase Deficiency Is Associated with Developmental Abnormalities
978 and Reduced Transmethylation." *Plant Physiology* 128 (3): 812–21.
979 https://doi.org/10.1104/pp.010880.
980 Murugan, Madhuvika, Denise Fedele, David Millner, Enmar Alharfoush, Geetasravya Vegunta, and
981 Detlev Boison. 2021. "Adenosine Kinase: An Epigenetic Modulator in Development and Disease."
982 *Neurochemistry International* 147 (July):105054. https://doi.org/10.1016/j.neuint.2021.105054.
983 Newby, Andrew C. 1984. "Adenosine and the Concept of 'Retaliatory Metabolites.'" *Trends in
984 Biochemical Sciences* 9 (2): 42–44. https://doi.org/10.1016/0968-0004(84)90176-2.
985 Novakova, Milena, and Tomas Dolezal. 2011. "Expression of Drosophila Adenosine Deaminase in
986 Immune Cells during Inflammatory Response." Edited by Pankaj Kapahi. *PLoS ONE* 6 (3): e17741.
987 https://doi.org/10.1371/journal.pone.0017741.
988 Parkhitko, Andrey A., Richard Binari, Nannan Zhang, John M. Asara, Fabio Demontis, and Norbert
989 Perrimon. 2016. "Tissue-Specific down-Regulation of S-Adenosyl-Homocysteine via Suppression
990 of dAhcyL1/dAhcyL2 Extends Health Span and Life Span in *Drosophila*." *Genes & Development* 30
991 (12): 1409–22. https://doi.org/10.1101/gad.282277.116.
992 Pedley, Anthony M., and Stephen J. Benkovic. 2017. "A New View into the Regulation of Purine
993 Metabolism: The Purinosome." *Trends in Biochemical Sciences* 42 (2): 141–54.
994 https://doi.org/10.1016/j.tibs.2016.09.009.
995 Peng, Wanling, Wu Zhaofa, Song Kun, Zhang Siyu, Li Yulong, Xu Min. 2020. "Regulation of sleep
996 homeostasis mediator adenosine by basal forebrain glutamatergic neurons." *Science* 369(6508):
997 eabb0556. https://doi.org/10.1126/science.abb0556.

998 Pike, M C, and C A DeMeester. 1988. “Inhibition of Phosphoinositide Metabolism in Human
999 Polymorphonuclear Leukocytes by S-Adenosylhomocysteine.” *Journal of Biological Chemistry*
1000 263 (8): 3592–99. https://doi.org/10.1016/S0021-9258(18)68966-5.
1001 Pike, M C, N M Kredich, and R Snyderman. 1978. “Requirement of S-Adenosyl-L-Methionine-Mediated
1002 Methylation for Human Monocyte Chemotaxis.” *Proceedings of the National Academy of*
1003 *Sciences* 75 (8): 3928–32. https://doi.org/10.1073/pnas.75.8.3928.
1004 Reiss, Allison B., David Grossfeld, Lora J. Kasselman, Heather A. Renna, Nicholas A. Vernice, Wendy
1005 Drewes, Justin Konig, Steven E. Carsons, and Joshua DeLeon. 2019. “Adenosine and the
1006 Cardiovascular System.” *American Journal of Cardiovascular Drugs* 19 (5): 449–64.
1007 https://doi.org/10.1007/s40256-019-00345-5.
1008 Roy, Dominic G., Jocelyn Chen, Victoria Mamane, Eric H. Ma, Brejnev M. Muhire, Ryan D. Sheldon,
1009 Tatiana Shorstova, et al. 2020. “Methionine Metabolism Shapes T Helper Cell Responses through
1010 Regulation of Epigenetic Reprogramming.” *Cell Metabolism* 31 (2): 250-266.e9.
1011 https://doi.org/10.1016/j.cmet.2020.01.006.
1012 Salminen, Antero, Juha M. T. Hyttinen, and Kai Kaarniranta. 2011. “AMP-Activated Protein Kinase
1013 Inhibits NF-κB Signaling and Inflammation: Impact on Healthspan and Lifespan.” *Journal of*
1014 *Molecular Medicine* 89 (7): 667–76. https://doi.org/10.1007/s00109-011-0748-0.
1015 Sbodio, Juan I, Solomon H Snyder, and Bindu D Paul. 2019. “Regulators of the Transsulfuration
1016 Pathway.” *British Journal of Pharmacology* 176 (4): 583–93. https://doi.org/10.1111/bph.14446.
1017 Schädlich, Ines Sophie, Riekje Winzer, Joschi Stabernack, Eva Tolosa, Tim Magnus, and Björn Rissiek.
1018 2023. “The Role of the ATP-Adenosine Axis in Ischemic Stroke.” *Seminars in Immunopathology*
1019 45 (3): 347–65. https://doi.org/10.1007/s00281-023-00987-3.
1020 Shimkets, Lawrence J., and Martin Dworkin. 1981. “Excreted Adenosine Is a Cell Density Signal for the
1021 Initiation of Fruiting Body Formation in Myxococcus Xanthus.” *Developmental Biology* 84 (1):
1022 51–60. https://doi.org/10.1016/0012-1606(81)90369-9.
1023 Singh, Sangita, Dominique Padovani, Rachel A. Leslie, Taurai Chiku, and Ruma Banerjee. 2009. “Relative
1024 Contributions of Cystathionine β-Synthase and γ-Cystathionase to H2S Biogenesis via Alternative
1025 Trans-Sulfuration Reactions.” *Journal of Biological Chemistry* 284 (33): 22457–66.
1026 https://doi.org/10.1074/jbc.M109.010868.
1027 Stenesen, Drew, Jae Myoung Suh, Jin Seo, Kweon Yu, Kyu-Sun Lee, Jong-Seok Kim, Kyung-Jin Min, and
1028 Jonathan M. Graff. 2013. “Adenosine Nucleotide Biosynthesis and AMPK Regulate Adult Life
1029 Span and Mediate the Longevity Benefit of Caloric Restriction in Flies.” *Cell Metabolism* 17 (1):
1030 101–12. https://doi.org/10.1016/j.cmet.2012.12.006.
1031 Straub, Rainer H. 2014. “Insulin Resistance, Selfish Brain, and Selfish Immune System: An Evolutionarily
1032 Positively Selected Program Used in Chronic Inflammatory Diseases.” *Arthritis Research &*
1033 *Therapy* 16 (S2): S4. https://doi.org/10.1186/ar4688.
1034 Vizán, Pedro, Luciano Di Croce, and Sergi Aranda. 2021. “Functional and Pathological Roles of AHCY.”
1035 *Frontiers in Cell and Developmental Biology* 9 (March):654344.
1036 https://doi.org/10.3389/fcell.2021.654344.
1037 Xu, Yiming, Yong Wang, Siyuan Yan, Qiuhua Yang, Yaqi Zhou, Xianqiu Zeng, Zhiping Liu, et al. 2017.
1038 “Regulation of Endothelial Intracellular Adenosine via Adenosine Kinase Epigenetically
1039 Modulates Vascular Inflammation.” *Nature Communications* 8 (1): 943.
1040 https://doi.org/10.1038/s41467-017-00986-7.
1041 Xuan, Mengjuan, Xinyu Gu, Juan Li, Di Huang, Chen Xue, and Yuting He. 2023. “Polyamines: Their
1042 Significance for Maintaining Health and Contributing to Diseases.” *Cell Communication and*
1043 *Signaling* 21 (1). https://doi.org/10.1186/s12964-023-01373-0.
1044 Yu, Weiwei, Zhen Wang, Kailian Zhang, Zhexu Chi, Ting Xu, Danlu Jiang, Sheng Chen, et al. 2019. “One-
1045 Carbon Metabolism Supports S-Adenosylmethionine and Histone Methylation to Drive

1046 Inflammatory Macrophages." *Molecular Cell* 75 (6): 1147-1160.e5.
1047 https://doi.org/10.1016/j.molcel.2019.06.039.
1048 Zeleznikar, R. J., R. A. Heyman, R. M. Graeff, T. F. Walseth, S. M. Dawis, E. A. Butz, and N. D. Goldberg.
1049 1990. "Evidence for Compartmentalized Adenylate Kinase Catalysis Serving a High Energy
1050 Phosphoryl Transfer Function in Rat Skeletal Muscle." *The Journal of Biological Chemistry* 265
1051 (1): 300–311.
1052 Zeleznikar, Robert J., Petras P. Dzeja, and Nelson D. Goldberg. 1995. "Adenylate Kinase-Catalyzed
1053 Phosphoryl Transfer Couples ATP Utilization with Its Generation by Glycolysis in Intact Muscle."
1054 *Journal of Biological Chemistry* 270 (13): 7311–19. https://doi.org/10.1074/jbc.270.13.7311.
1055 Zimmerman, Thomas P., Gerald Wolberg, and Gail S. Duncan. 1978. "Inhibition of Lymphocyte-Mediated
1056 Cytolysis by 3-Deazaadenosine: Evidence for a Methylation Reaction Essential to Cytolysis."
1057 *Proceedings of the National Academy of Sciences* 75 (12): 6220–24.
1058 https://doi.org/10.1073/pnas.75.12.6220.
1059